Applied Problems of Physics and Mathematics

Integrated Defect Engineering in Perovskite Solar Cells for Enhanced Stability and Efficiency

Kubakova Aizada[1], Chen Xinlei[2]
Osh Technological Univercity, Str. N.Isanov, 81, Osh 723503, Kyrgyzstan
aizadakubakova@gmail.com, SPP659hv@gmail.com

Abstract: This study presents a comprehensive analysis of defect engineering strategies in perovskite solar cells (PSCs) aimed at improving device stability and power conversion efficiency. Particular attention is given to three key approaches: chemical passivation using organic and inorganic additives, structural control of crystallization and perovskite film morphology, and interfacial engineering through the incorporation of interfacial barriers and dipole layers. Experimental results and numerical simulations demonstrate that the synergistic implementation of these strategies significantly reduces trap-state density and suppresses non-radiative recombination pathways, thereby enhancing the open-circuit voltage (VOS) and fill factor (FF).

Stability tests conducted under international ISOS protocols indicate that defect-engineered devices retained more than 85–90% of their initial power conversion efficiency after 1000 h of operation, whereas reference devices exhibited a performance loss exceeding 50% under comparable conditions. Scanning electron microscopy analysis revealed improved film compactness, reduced grain-boundary discontinuities, and fewer visible morphological defects. In parallel, modelling results confirmed an exponential correlation between defect density and the degradation dynamics of VOS and F.

Furthermore, the scalability of deposition techniques, including blade coating, slot-die coating, and roll-to-roll processing, demonstrated the reproducibility of defect-engineering effects during the transition from small-area laboratory devices to larger-area modules. Nevertheless, challenges associated with film uniformity, long-term environmental stability, and process reproducibility remain to be fully addressed. Overall, the findings suggest that the integration of chemical, structural, and interfacial defect engineering provides a universal and effective strategy for simultaneously increasing PSC efficiency by 12–15% and substantially improving operational stability. These results open promising prospects for the industrial implementation of perovskite photovoltaic technologies and their integration into tandem solar-cell architectures, contributing to the advancement of renewable energy systems and the achievement of sustainable development goals.

Keywords: Perovskite solar cells; defect engineering; passivation; interfacial engineering; operational stability; power conversion efficiency; scalability; renewable energy; open-circuit voltage; fill factor.

1. Introduction

1.1. Relevance of Perovskite Solar Cells

Over the past two decades, renewable energy has become not only a strategic priority of global energy policy but also one of the central directions of advanced scientific research [1]. Among emerging photovoltaic technologies, perovskite solar cells (PSCs) have attracted particular attention due to their rapid progress in power conversion efficiency. Since their first demonstration with efficiencies below 4% in 2009, PSCs have achieved certified efficiencies exceeding 26% by 2023 [2]. This remarkable improvement positions perovskite-based photovoltaic materials among the most promising candidates for either complementing or partially replacing conventional silicon solar cells.

Despite this outstanding progress, the commercial deployment of PSCs remains limited by fundamental challenges related to material instability and device degradation [3]. The most vulnerable regions within PSC architectures include grain boundaries, interfacial layers, crystal-lattice imperfections, and ion-migration pathways. These factors collectively accelerate non-radiative recombination, charge-transport imbalance, phase instability, and interfacial degradation, ultimately resulting in reduced operational stability and efficiency loss [4].

Defect engineering has therefore emerged as a critical approach for addressing the intrinsic and extrinsic limitations of perovskite photovoltaic devices. By controlling defect formation, passivating trap states, improving film crystallinity, and stabilizing interfaces, it becomes possible to enhance both the photovoltaic performance and long-term durability of PSCs. In this context, the present study focuses on the combined role of chemical passivation, structural optimization, and

interfacial engineering as an integrated strategy for improving the stability and efficiency of perovskite solar cells.

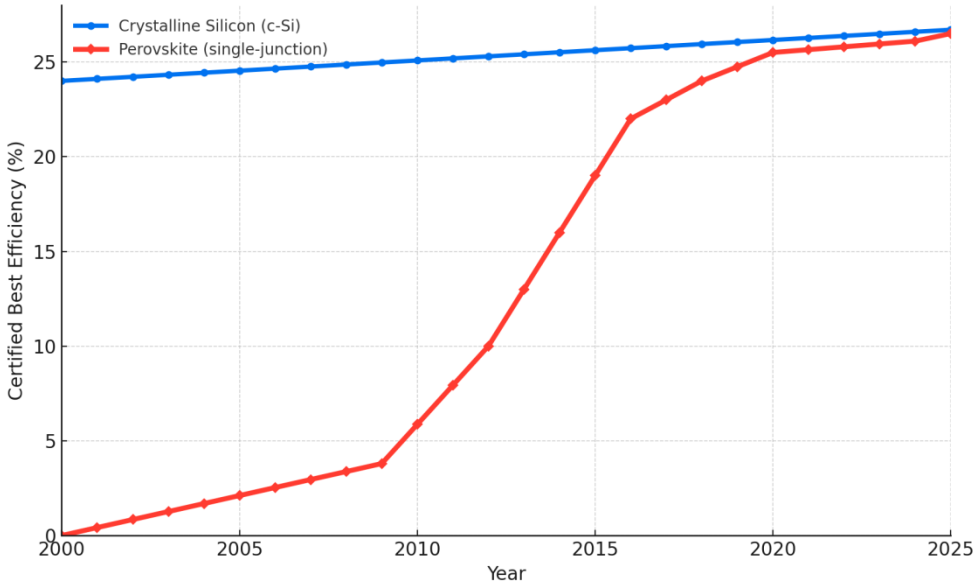

Figure 1. Comparative Evolution of Power Conversion Efficiency in Crystalline Silicon and Perovskite Solar Cells from 2000 to 2025

Figure 1 schematically compares the evolution of certified best power conversion efficiency values for two photovoltaic technologies between 2000 and 2025: crystalline silicon solar cells (c-Si) and single-junction perovskite solar cells (PSCs). The data should be presented using certified or independently confirmed record efficiencies, preferably based on internationally recognized efficiency charts and reports. Such an approach is essential for ensuring the reliability and comparability of the plotted values across different photovoltaic technologies.

The first curve illustrates the gradual improvement of crystalline silicon devices. Silicon solar cells started from a relatively high efficiency baseline and have demonstrated a slow but steady increase over time. This improvement has mainly been associated with advances in wafer quality, surface texturing, surface and interface passivation, light-management strategies, and improved contact architectures. In contrast to emerging photovoltaic technologies, the efficiency trajectory of crystalline silicon is relatively smooth and approaches a technological saturation regime.

The second curve represents the rapid development of single-junction perovskite solar cells. Unlike silicon, PSCs exhibited a remarkably steep efficiency increase after their initial low-efficiency demonstrations in 2009. This rapid progress has been driven by improvements in perovskite composition, mixed-cation and mixed-halide engineering, chemical defect passivation, crystallization control, and interfacial optimization. The visual contrast between the two curves highlights the central message of the figure: perovskite solar cells have achieved efficiency levels comparable to mature silicon technologies within a much shorter development period.

For an international readership, the figure should include English axis labels, a clear legend, and a concise explanation of data origin. The recommended axis labels are **“Year”** for the x-axis and **“Certified Power Conversion Efficiency (%)”** for the y-axis. The legend may include **“Crystalline silicon solar cells”** and **“Single-junction perovskite solar cells”**. The figure should also make clear that, although perovskites have demonstrated exceptionally rapid efficiency progress, their long-term operational stability, environmental durability, and large-area scalability remain critical challenges for commercialization.

Table 1 summarizes the principal defect types commonly observed in perovskite solar cells and their expected influence on key photovoltaic parameters, including open-circuit voltage (VOS), short-circuit current density (JSC), and fill factor (FF). Both point defects, such as vacancies and interstitial ions, and extended or morphology-related defects, such as grain-boundary states, are considered.

Each defect type is associated with a characteristic energetic position within or near the bandgap, which determines its ability to trap charge carriers and participate in recombination processes.

Iodine vacancies (VI) are often discussed as shallow donor-like defects that may influence ion migration and interfacial instability, particularly at surfaces and grain boundaries. However, their role as direct non-radiative recombination centers should be treated cautiously, since recent studies indicate that the recombination activity of VIV depends strongly on its position, structural configuration, and local chemical environment. By contrast, lead vacancies (VPb) are frequently associated with deeper acceptor-like states and can contribute more directly to trap-assisted recombination and VOS losses.

Special attention should be given to grain-boundary states and oxygen-related defects. Grain boundaries can accumulate undercoordinated ions, residual precursor species, and mobile defects, thereby acting as preferred pathways for ion migration and environmental degradation. Oxygen-related defects may form under illumination in the presence of oxygen and moisture, accelerating photo-oxidation and leading to a progressive decline in F, JSC, and operational stability.

Overall, the data summarized in Table 1 confirm the central role of defect engineering in the development of reliable perovskite solar cells. Reducing defect concentration, suppressing defect-assisted recombination, and stabilizing interfaces are essential requirements for achieving high efficiency, low hysteresis, and long-term operational durability.

Lead vacancy defects in MAPbI3 have been experimentally identified using positron annihilation lifetime spectroscopy supported by density functional theory, and such defects have been associated with deep-level hole trapping. At the same time, recent work on iodine vacancies shows that their impact is not universal and depends on surface position and defect configuration, which is why the wording in the table was made more cautious.

3. Strategies for Defect Engineering

Modern defect-engineering approaches in perovskite solar cells can be classified into several complementary categories.

First, **chemical passivation** involves the incorporation of passivating agents capable of coordinating undercoordinated ions, filling vacancy-related sites, and reducing the density of electronically active trap states. Examples include thiocyanate-based compounds, Lewis bases, ammonium salts, guanidinium-containing additives, fullerene derivatives, and multifunctional organic molecules. These additives can suppress non-radiative recombination, improve carrier lifetime, and enhance the open-circuit voltage of PSCs [7].

Second, **nanostructuring and interfacial engineering** are used to modify grain boundaries, improve film morphology, and regulate charge transfer at the interfaces between the perovskite absorber and charge-transport layers. Such strategies include surface treatment, buried-interface passivation, insertion of ultrathin buffer layers, dipole-layer engineering, and the use of two-dimensional or quasi-two-dimensional perovskite layers. These approaches reduce interfacial trap density, suppress charge accumulation, and improve both device efficiency and stability [8].

Third, **cation and anion compositional engineering** enables the stabilization of the perovskite lattice and the reduction of defect-assisted degradation. Partial substitution of A-site cations, such as methylammonium (MA+), formamidinium (FA+), cesium (Cs+), or rubidium (Rb+), can improve phase stability and crystallinity. Halide engineering through controlled incorporation of iodide, bromide, or chloride can tune the bandgap and influence ion migration. However, mixed-halide systems must be carefully optimized because excessive halide segregation may reduce photostability under illumination [9].

Fourth, **device-architecture optimization** involves the design of multilayer structures and barrier layers that prevent moisture ingress, oxygen diffusion, metal-electrode migration, and interfacial chemical reactions. Appropriate electron-transport layers, hole-transport layers, self-assembled monolayers, hydrophobic interlayers, and encapsulation strategies can substantially improve

operational durability. In this regard, device architecture is not only a charge-transport framework but also a key component of defect and degradation management [10].

Taken together, these approaches demonstrate that effective defect engineering requires a synergistic strategy rather than a single isolated modification. Chemical passivation reduces the density of trap states, structural control improves film crystallinity and morphology, compositional engineering stabilizes the perovskite lattice, and interfacial engineering suppresses charge recombination and environmental degradation. The integration of these strategies provides a promising route toward high-efficiency, stable, and scalable perovskite photovoltaic technologies.

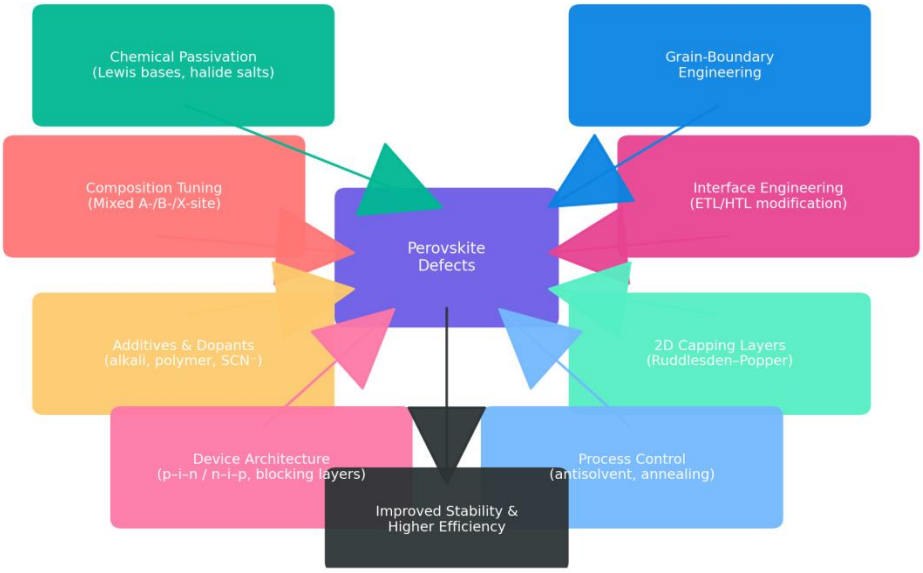

Figure 2. Schematic Illustration of Defect-Engineering Strategies in Perovskite Solar Cells

Figure 2 schematically illustrates the major defect-engineering strategies employed in perovskite solar cells and their targeted effects on defect states within the photoactive absorber layer. At the center of the scheme, the core block “Perovskite Defects” represents the main defect-related limitations, including trap states, undercoordinated ions, ion-migration pathways, grain-boundary defects, and interfacial recombination centers.

Several complementary approaches are directed toward this central defect block. Chemical passivation, involving Lewis bases, Lewis acids, halide salts, ammonium-based molecules, and multifunctional organic additives, is used to coordinate undercoordinated ions and reduce the density of electronically active trap states. Compositional engineering, including mixed-cation and mixed-anion substitution at the A, B, and X sites of the perovskite lattice, is employed to tune lattice stability, suppress phase segregation, and improve defect tolerance. Interfacial engineering, based on the modification of electron-transport layers (ETLs), hole-transport layers (HTLs), and buried or top interfaces, is designed to reduce interfacial recombination, optimize energy-level alignment, and facilitate selective charge extraction.

In addition, the scheme highlights the role of additive and dopant engineering, grain-boundary passivation, and process control. Processing strategies such as antisolvent treatment, solvent engineering, controlled annealing, atmosphere regulation, and crystallization-rate management are essential for obtaining compact, uniform, and highly crystalline perovskite films. Grain-boundary passivation reduces localized trap-state density and suppresses ion migration along extended defect pathways. Meanwhile, the deposition of two-dimensional capping layers, including Ruddlesden–Popper-type structures, can protect the perovskite surface, improve moisture and thermal resistance, and reduce non-radiative recombination at surface and interfacial regions.

The lower part of the scheme emphasizes the final target of defect engineering: the simultaneous achievement of enhanced operational stability and higher power conversion efficiency. These strategies do not act independently but rather function synergistically. For example, combining

compositional engineering with two-dimensional capping layers and interfacial modification can simultaneously reduce trap density and trap depth, improve charge transport, suppress ion migration, and increase tolerance to humidity, oxygen, light, and heat. Therefore, integrated compositional, structural, and interfacial control represents a fundamental toolkit for translating laboratory-scale advances in perovskite solar cells into long-term operational devices and scalable industrial photovoltaic modules.

Suggested improved transition to the next section

To establish a reliable correlation between defect-engineering strategies and device performance, it is necessary to evaluate not only the initial photovoltaic parameters but also their temporal evolution under standardized operational conditions. In the following section, the effects of defect density on VOS, JSC, F and long-term degradation kinetics are examined in detail.

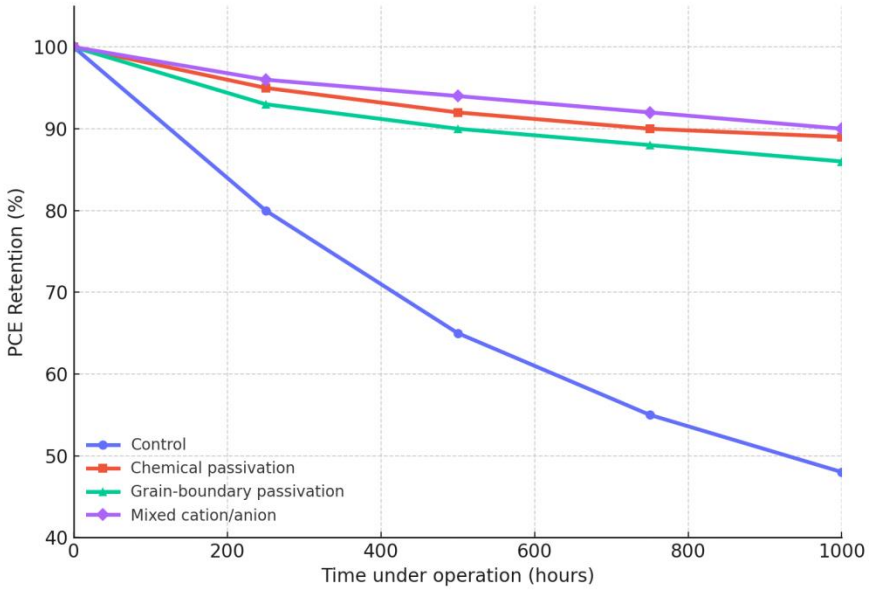

Figure 3. Power Conversion Efficiency Retention of Perovskite Solar Cells during Operation under Different Defect-Engineering Strategies

Figure 3 illustrates the evolution of power conversion efficiency retention (PCE Retention) in perovskite solar cells as a function of operating time for devices fabricated with different defect-engineering approaches. The graph highlights the substantial difference in long-term performance between untreated control devices and those incorporating defect-passivation and defect-management strategies.

The control sample, which did not undergo any deliberate defect passivation or structural optimization, exhibits rapid degradation during operation. By 1000 h of continuous testing, the control device retains less than 50% of its initial power conversion efficiency. This pronounced decline is mainly associated with ion migration, degradation at grain boundaries, interfacial instability, and the progressive increase in non-radiative recombination centers. The steep downward trajectory of the **"Control"** curve clearly emphasizes the intrinsic instability of unmodified perovskite structures.

In contrast, devices incorporating defect-engineering strategies demonstrate markedly improved stability. Approaches such as **chemical passivation**, **grain-boundary modification**, and **mixed cation/anion compositional engineering** enable the devices to retain approximately 90% of their initial efficiency after 1000 h of operation. The more gradual degradation profiles of these curves indicate that the reduction of trap-state density, improvement of film morphology, and suppression of ion diffusion play a decisive role in extending device lifetime.

This figure therefore provides clear visual evidence that defect engineering is not merely an auxiliary optimization strategy, but rather a fundamental tool for enhancing the operational reliability of perovskite solar cells. By mitigating non-radiative recombination and stabilizing both bulk and

interfacial properties, defect-engineered devices achieve a substantially improved balance between efficiency and durability.

Figure 4. Comparative Analysis of Challenges and Solutions in Defect Engineering for Perovskite Solar Cells

Figure 4 presents a problem–solution tree that systematically summarizes the major challenges and corresponding solutions in defect engineering for perovskite solar cells. The upper part of the diagram contains the central block “Challenges in Defect Engineering”, from which three main branches emerge: chemical engineering, structural control, and scalability. Each branch represents a distinct level at which defects influence the performance and durability of perovskite photovoltaic devices.

The first branch, chemical engineering, addresses defect-related issues such as deep trap states, halide and metal vacancies, undercoordinated ions, and chemically unstable surface sites. These defects are commonly associated with trap-assisted non-radiative recombination, reduced open-circuit voltage, enhanced ion migration, and accelerated degradation under operational stress. Corresponding solutions include the use of passivating agents, Lewis bases and acids, halide salts, ammonium-based additives, multifunctional organic molecules, and dopants capable of stabilizing the perovskite lattice and reducing the density of electronically active defects.

The second branch, structural control, focuses on morphology-related defects, including grain-boundary states, pinholes, local phase inhomogeneity, poor crystallinity, and non-uniform film formation. These structural imperfections create pathways for moisture penetration, ion migration, and interfacial degradation. Possible solutions include grain-boundary passivation, optimization of crystallization kinetics, controlled annealing, antisolvent engineering, solvent coordination strategies, and the incorporation of hybrid two-dimensional/three-dimensional (2D/3D) perovskite structures. In particular, Ruddlesden–Popper-type 2D layers can act as protective capping structures that suppress surface recombination and improve resistance to humidity and thermal stress.

The third branch, scalability, highlights the challenges associated with transferring laboratory-scale high-efficiency devices to industrially relevant large-area modules. These challenges include film uniformity over large substrates, reproducibility of defect passivation, compatibility with high-throughput manufacturing, long-term process stability, and minimization of material waste. Potential solutions involve scalable coating and printing methods such as blade coating, slot-die coating, spray coating, inkjet printing, and roll-to-roll processing.

In the lower part of the diagram, these solutions converge into integrated defect-engineering strategies, including compositional tuning, interfacial modification, device-architecture optimization, and scalable process control. The final target of these strategies is the development of stable and high-efficiency perovskite solar cells suitable for long-term operation and industrial implementation. Overall, the diagram emphasizes that defect engineering is inherently multidimensional: defects originate not only within the perovskite bulk but also at grain boundaries, interfaces, surfaces, and during large-area processing.

2. Materials and Methods

2.1. Experimental Design

2.1.1. General Experimental Workflow

A comprehensive experimental design was employed in this study to evaluate the role of defect engineering in improving the stability and efficiency of perovskite solar cells. The workflow included the synthesis of thin-film perovskite absorbers, controlled modification of defect states, morphological and structural characterization, and electrical and optical performance measurements. The experimental strategy was designed to compare reference devices with defect-engineered devices fabricated under comparable conditions. This approach made it possible to determine the influence of chemical passivation, compositional modification, interface engineering, and crystallization control on the photovoltaic parameters and degradation behavior of the devices.

The main focus was placed on hybrid organic–inorganic perovskite systems, particularly methylammonium lead iodide (CH3NH3PbI3) and mixed-cation perovskites based on cesium, formamidinium, and methylammonium (Cs/FA/MA). These compositions were selected because they combine strong optical absorption, tunable bandgap properties, relatively high power conversion efficiency, and potential compatibility with tandem photovoltaic architectures [12].

In addition, mixed-cation systems were considered especially relevant for stability-oriented studies, since compositional engineering can improve phase stability, suppress undesirable lattice distortion, and reduce the formation of defect-assisted degradation pathways. The comparison between single-cation and mixed-cation perovskite films enabled a more detailed evaluation of how compositional complexity affects defect formation, carrier recombination, and operational durability.

2.1.2. Thin-Film Deposition and Device Architecture

Perovskite thin films were deposited using a spin-coating method combined with a controlled antisolvent-assisted crystallization process. After deposition, the films were subjected to thermal annealing in order to promote crystallization, enhance grain growth, and improve film compactness. The antisolvent step was used to control supersaturation during film formation and to obtain uniform perovskite layers with reduced pinhole density and improved surface coverage.

The device architecture included electron-transport layers (ETLs), perovskite absorber layers, hole-transport layers (HTLs), and metal electrodes. Titanium dioxide (T_iO_2) and tin dioxide (S_nO_2) were employed as electron-transport layers, while Spiro-OMeTAD and PTAA were used as hole-transport materials [13]. These transport layers were selected because of their established compatibility with high-performance perovskite solar-cell architectures and their ability to influence charge extraction, interfacial recombination, and device stability.

The use of different ETL and HTL materials also enabled the evaluation of interfacial effects on defect formation and charge-transport behavior. In particular, S_nO_2-based ETLs are often preferred in low-temperature processing and tandem-compatible architectures, whereas T_iO_2-based ETLs provide a conventional reference system for comparison. Similarly, Spiro-OMeTAD and PTAA offer different interfacial properties, which can influence hole extraction, interfacial recombination losses, and long-term operational stability.

To investigate the effect of defect engineering, selected devices were modified using passivating additives, compositional tuning, grain-boundary treatment, or interfacial modification. The resulting

films and devices were compared with untreated reference samples in terms of morphology, crystallinity, photovoltaic performance, hysteresis behavior, and stability under accelerated aging or operational testing conditions.

Perovskite solar cells were fabricated using a controlled thin-film deposition protocol based on spin coating, antisolvent-assisted crystallization, and subsequent thermal annealing. The investigated absorber compositions included CH3NH3PbI3 and mixed-cation Cs/FA/MA-based perovskites, selected for their high photovoltaic performance and relevance to tandem solar-cell architectures. Electron-selective contacts were prepared using T_iO_2 or S_nO_2, whereas Spiro-OMeTAD and PTAA were employed as hole-transport layers. Defect-engineered samples were prepared by introducing chemical passivating agents, compositional modifiers, grain-boundary treatments, and interfacial layers. Reference devices without intentional defect modification were fabricated under identical processing conditions to enable a direct comparison of morphology, defect density, charge recombination, photovoltaic performance, and operational stability.

Table 1. Important note for completing the Methods section

Parameter	Required detail for
Perovskite precursor	Exact molar concentration, solvent system, precursor ratio
Spin-coating process	Rotation speed, time, acceleration, antisolvent type and dripping time
Annealing	Temperature, duration, atmosphere
ETL/HTL deposition	Material concentration, deposition method, annealing or oxidation conditions
Defect passivator	Chemical name, concentration, introduction route
Device area	Active area and aperture area
Characterization	SEM, XRD, PL/TRPL, UV–Vis, J–V, EQE, EIS, SCLC
Stability testing	ISOS protocol, temperature, humidity, illumination intensity, atmosphere
Statistics	Number of devices, average PCE, standard deviation, champion device

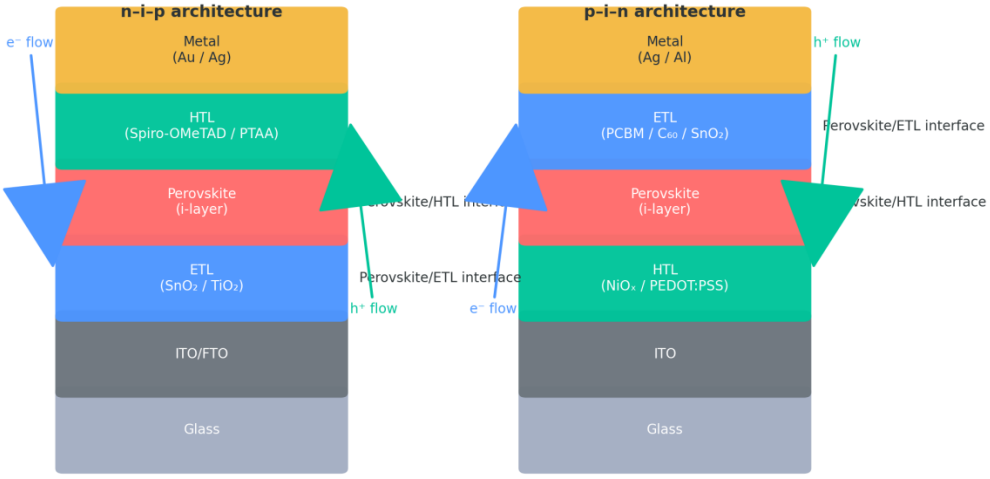

Figure 5. Schematic Architecture of n–i–p and p–i–n Perovskite Solar Cells

Figure 5 schematically illustrates two widely used device architectures in perovskite solar cells: the conventional **n–i–p** configuration and the inverted **p–i–n** configuration. The scheme clearly identifies the position of the photoactive perovskite absorber layer, denoted as the intrinsic layer (i-layer), as well as the critical interfacial regions between the perovskite and charge-transport layers.

In the **n–i–p architecture**, the layer sequence from the transparent substrate to the top electrode is typically arranged as follows:

Glass/ITO(FTO)→ETL→Perovskite→HTL→Metal electrode.}

→ETL→Perovskite→HTL→Metal electrode.

In this configuration, tin oxide (S_nO_2) or titanium dioxide (TiO2) is commonly used as the electron-transport layer (ETL), while Spiro-OMeTAD or PTAA is employed as the hole-transport layer (HTL). The metallic top electrode is usually based on gold (Au), silver (Ag), or other conductive materials compatible with the selected device stack.

In the **p–i–n architecture**, the order of the charge-selective layers is inverted:

Glass/ITO→HTL→Perovskite→ETL→Metal electrode.

Here, nickel oxide (NiOx), PEDOT:PSS, or self-assembled monolayers may serve as hole-selective layers, whereas fullerene-based materials such as PCBM and C_{60}, often combined with S_nO_2, are used as electron-selective contacts. The top electrode is commonly Ag, Al, Cu, or another low-resistance metal contact.

The arrows in the scheme indicate the direction of charge transport. Electrons are selectively extracted through the ETL, while holes are transported through the HTL toward the opposite electrode. The relative position of the ETL and HTL determines the direction of carrier extraction and strongly affects interfacial recombination, energy-level alignment, hysteresis behavior, and operational stability.

Special attention is given to the **Perovskite/ETL** and **Perovskite/HTL** interfaces, since these regions are among the most critical sites for defect formation and defect passivation. Interfacial defects can originate from undercoordinated ions, energy-level mismatch, chemical incompatibility, residual precursor species, local strain, and charge accumulation. Such defects promote non-radiative recombination, reduce V_{OS}, increase hysteresis, and accelerate long-term degradation.

The comparison between n–i–p and p–i–n structures highlights that each architecture requires a specific interfacial-engineering strategy. In n–i–p devices, particular emphasis is placed on transparent oxide-based ETLs and stable organic HTLs. In contrast, p–i–n devices benefit from robust inorganic or molecular HTLs, such as N_iO_x or self-assembled monolayers, and fullerene-based ETLs, which can improve electron extraction and reduce interfacial recombination. Therefore, visualizing both architectures provides a useful framework for comparing defect-engineering strategies aimed at minimizing trap density at the corresponding buried and top interfaces.

2.2. Chemical Engineering

2.2.1. Compositional Optimization and Alkali-Metal Cation Incorporation

To reduce the density of intrinsic defects and improve lattice stability, the stoichiometry of perovskite precursors was carefully optimized. Particular attention was given to controlling the ratio between organic or inorganic cations, lead halides, and halide components, since even small deviations from stoichiometry can promote the formation of vacancies, interstitial defects, secondary phases, and trap states.

The incorporation of alkali-metal cations, such as Cs+ and Rb+, was used as a compositional-engineering strategy to stabilize the perovskite crystal lattice and suppress phase instability [14]. These cations can influence crystallization kinetics, lattice tolerance factors, grain formation, and defect distribution. In mixed-cation perovskites, partial incorporation of Cs+ and Rb+ may improve phase uniformity and reduce the formation of defect-rich domains. However, their concentration must be carefully optimized, since excessive alkali-metal incorporation may lead to phase segregation, altered band alignment, or reduced charge transport.

Thus, compositional optimization was considered not only as a method for improving the crystallographic stability of the absorber layer, but also as a route for reducing defect-assisted recombination and improving device reproducibility.

2.2.2. Molecular Additives and Defect Passivation

Molecular additives were introduced to passivate undercoordinated ions, suppress trap-assisted non-radiative recombination, and improve perovskite film morphology. Additives such as ammonium thiocyanate, guanidinium-containing compounds, and polyethyleneimine were selected because of their ability to interact with ionic defects, surface states, and grain-boundary trap sites [15].

Ammonium thiocyanate (NH4SCN) can influence crystallization and coordinate with undercoordinated Pb2+ species through the thiocyanate group, thereby reducing the density of surface and grain-boundary traps. Guanidinium cations (C(NH2)3+) can contribute to lattice stabilization through hydrogen bonding and partial incorporation or surface interaction at A-site-related defect regions. Polyethyleneimine (PEI), which contains multiple amine groups, can interact with undercoordinated lead ions and modify interfacial energy alignment, although excessive polymer loading may introduce insulating barriers and hinder charge extraction.

Overall, the use of molecular additives provides a flexible approach for defect passivation. Their effectiveness depends on chemical structure, concentration, spatial distribution, compatibility with the perovskite precursor system, and the resulting influence on crystallization and interfacial charge transport.

Table 2. Additives Used for Defect Passivation and Their Proposed Mechanisms of Action

Additive	Target defect or affected region	Proposed passivation mechanism
Ammonium thiocyanate (NH4SCN)	Undercoordinated Pb2+, Pb-related surface defects, grain-boundary traps	Coordination of SCN− with undercoordinated Pb2+; modulation of crystallization; reduction of trap density and non-radiative recombination losses
Guanidinium (C(NH2)3+)	A-site-related defects, surface defects, lattice instability	Hydrogen bonding and partial A-site or surface interaction; stabilization of the perovskite lattice; suppression of defect-assisted degradation
Polyethyleneimine (PEI)	Perovskite surface and grain boundaries	Amine-group coordination with undercoordinated metal ions; passivation of grain-boundary traps; modification of interfacial energy-level alignment
Potassium chloride (KCl)	Perovskite surface, halide-vacancy-related defects, grain boundaries	K+-assisted passivation of halide-related defects; improved crystallinity and film uniformity; suppression of ion migration
Poly(methyl methacrylate) (PMMA)	Surface and interfacial regions	Formation of a thin protective polymer layer; suppression of ion diffusion; reduction of contact-

		induced defects and environmental degradation
3-Aminopropyltriethoxysilane (APTES)	Perovskite/ETL interface	Formation of chemical bridging interactions between layers; reduction of interfacial trap density; improved interfacial adhesion and charge extraction

Note: The mechanisms listed in Table 2 should be interpreted as proposed or dominant mechanisms. The actual effect of each additive depends on concentration, processing conditions, perovskite composition, device architecture, and the position of the additive within the film or interface.

Table 2 summarizes the additives used for defect passivation in perovskite solar cells, together with their target regions and proposed mechanisms of action. Each additive is directed toward specific defect types or structurally vulnerable regions. For example, ammonium thiocyanate can coordinate with undercoordinated lead species and reduce trap-assisted recombination, whereas guanidinium-based additives can stabilize the lattice through hydrogen bonding and A-site-related interactions. In this way, chemical additives provide a versatile tool for controlling perovskite composition, defect chemistry, crystallization behavior, and film morphology.

Polymeric and organosilane additives are particularly important for surface and interfacial passivation. PMMA can form a thin protective layer that suppresses ion diffusion and reduces direct chemical interaction between the perovskite and adjacent charge-transport materials. Similarly, 3-aminopropyltriethoxysilane can improve interfacial adhesion and create chemical bridging interactions at the Perovskite/ETL interface, thereby reducing interfacial trap density and improving device robustness.

The combined use of molecular, ionic, polymeric, and organosilane additives demonstrates that chemical engineering remains one of the most powerful strategies for enhancing both the efficiency and operational stability of perovskite solar cells. Nevertheless, additive concentration must be carefully optimized, since excessive passivation can introduce charge-transport barriers, modify crystallization unfavorably, or cause phase separation.

2.3. Structural Control

2.3.1. Crystallization Control, Grain-Boundary Passivation, and 2D Capping Layers

To reduce defect density at grain boundaries and improve the structural quality of perovskite films, several structural-control strategies were employed. These included slowed crystallization, controlled thermal annealing, solvent and antisolvent engineering, and the deposition of two-dimensional capping layers. Such approaches are designed to regulate nucleation and grain growth, improve film coverage, reduce pinhole formation, and suppress the formation of defect-rich grain-boundary regions.

Controlled crystallization plays a decisive role in determining the final morphology of the perovskite absorber. Rapid and uncontrolled crystallization often results in small grains, incomplete surface coverage, non-uniform thickness, and a high density of grain-boundary defects. In contrast, moderated crystallization kinetics can promote the formation of larger grains, improved compactness, and reduced surface roughness. This directly contributes to lower trap density, reduced non-radiative recombination, and improved charge-carrier transport.

Grain-boundary passivation was further enhanced through the incorporation of suitable organic cations and surface-treatment agents. In particular, two-dimensional capping layers based on phenethylammonium (PEA+) or related bulky organic ammonium cations can form Ruddlesden–Popper-type perovskite structures at the surface of the three-dimensional perovskite absorber [16].

These 2D layers can reduce surface trap density, suppress ion migration, improve moisture resistance, and protect the underlying 3D perovskite from environmental degradation.
However, the thickness and orientation of the 2D capping layer must be carefully controlled. A thin and well-oriented 2D layer can improve surface passivation and stability without significantly hindering charge extraction. By contrast, an excessively thick or poorly oriented 2D layer may increase transport resistance and reduce the fill factor. Therefore, structural control requires optimization of both defect passivation and charge-transport continuity.

2.3.2. Morphological Characterization by SEM and AFM

The morphology of the perovskite films was investigated using scanning electron microscopy (SEM) and atomic force microscopy (AFM). SEM analysis was used to evaluate surface coverage, grain size, compactness, pinhole density, and the presence of visible morphological defects. Both top-view and cross-sectional SEM images can provide valuable information on film continuity, layer thickness, and interfacial contact quality.
AFM measurements were performed to analyze surface roughness and nanoscale topography. Parameters such as root-mean-square roughness (Rq) and average roughness (Ra) were used to quantify the effect of defect-engineering strategies on film smoothness and uniformity. Lower surface roughness is generally beneficial for forming high-quality interfaces with charge-transport layers, reducing local electric-field concentration, and improving device reproducibility.
The combined use of SEM and AFM allowed a more complete assessment of how structural-control strategies influence perovskite film formation. Films treated with crystallization-control methods and 2D capping layers are expected to show improved grain connectivity, reduced pinhole density, smoother surfaces, and fewer defect-rich regions. These morphological improvements are directly related to enhanced charge transport, reduced recombination losses, and improved operational stability.

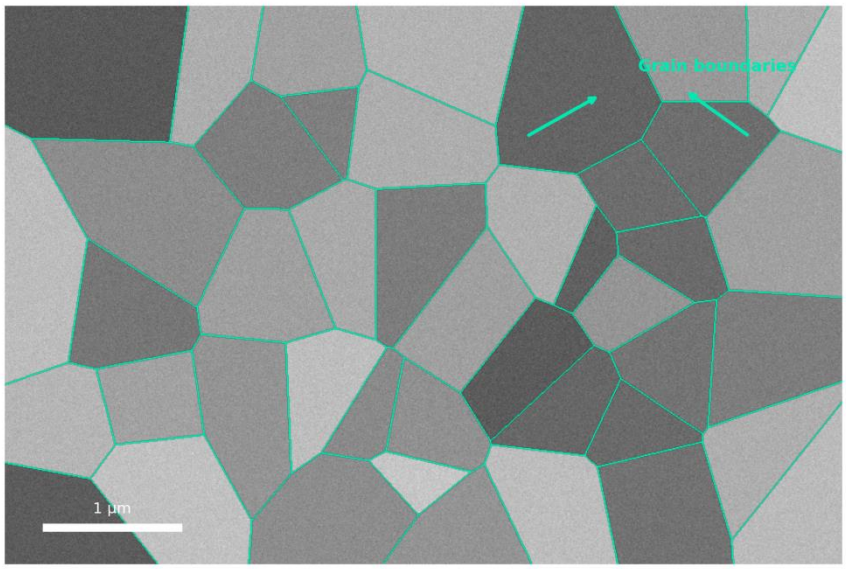

Figure 6. Simulated SEM-like Micrograph of a Perovskite Film with Highlighted Grain Boundaries

Figure 6 illustrates the microstructure of a perovskite thin film in the form of a simulated SEM-like image with clearly highlighted grain boundaries. Different grey-scale regions represent individual perovskite grains, while the bright contours indicate intergranular boundaries. These grain-boundary regions are commonly considered structurally vulnerable sites where defect accumulation, ion migration, and non-radiative recombination may occur.
A schematic scale bar of 1 μm is included to provide an approximate reference for the characteristic grain size and to relate the observed morphology to film-engineering parameters. The English

annotation “Grain boundaries” identifies the critical microstructural regions without overloading the image with excessive textual information.

Highlighting the grain boundaries makes it possible to visually localize regions where defect-engineering strategies, such as chemical passivation, controlled crystallization, or two-dimensional capping, can be effectively applied. Grain boundaries often contain undercoordinated ions, residual precursor species, local strain, and defect-rich domains, all of which can contribute to trap-assisted recombination and accelerated degradation.

This visualization also provides a useful framework for correlating film morphology with the electrical performance of perovskite solar cells. In general, an increased average grain size, improved grain connectivity, reduced pinhole density, and a lower total grain-boundary length are associated with reduced recombination losses, higher open-circuit voltage (VOS), improved fill factor (FF), and enhanced long-term operational stability. Therefore, grain-boundary engineering remains a key component of structural defect control in high-performance perovskite photovoltaic devices.

2.4. Interface Engineering

Interface engineering was employed to reduce interfacial trap density, improve energy-level alignment, suppress ion migration, and enhance the long-term stability of perovskite solar cells. Since the Perovskite/ETL and Perovskite/HTL interfaces strongly influence charge extraction, recombination dynamics, hysteresis behavior, and degradation pathways, targeted interfacial modification is essential for achieving high-performance and durable devices.

2.4.1. Surface Modification of the Electron-Transport Layer

The surface of the electron-transport layer, particularly S_nO_2, was modified using chloride- and fluoride-containing treatments in order to reduce surface defect states and improve interfacial contact with the perovskite absorber. Such treatments can passivate undercoordinated metal sites, hydroxyl-related surface groups, and oxygen-vacancy-related defects on the S_nO_2 surface.

Modification of the ETL surface can also influence perovskite nucleation and crystallization at the buried interface. A more chemically uniform and defect-passivated S_nO_2 surface promotes improved film coverage, reduced interfacial recombination, and more efficient electron extraction. In addition, halide- or fluoride-based surface treatment may help suppress charge accumulation at the buried interface, thereby reducing current–voltage hysteresis and improving operational reproducibility.

However, the concentration and processing conditions of the surface modifiers must be carefully optimized. Excessive ionic treatment may introduce unwanted interfacial dipoles, alter energy-level alignment, or create additional charge-transport barriers. Therefore, ETL surface modification should be considered an optimization tool that requires precise control over chemical composition, surface coverage, and interface energetics.

2.4.2. Organic Interlayers for Energy-Level Alignment

Organic interlayers were introduced to improve energy-level alignment between the perovskite absorber and the adjacent charge-transport layers. These ultrathin interfacial layers can create molecular dipoles, tune the work function of transport layers, reduce energetic mismatch, and suppress interfacial charge recombination.

Such interlayers are particularly useful when the conduction or valence band positions of the transport layers are not ideally matched with the perovskite absorber. By adjusting the interfacial dipole and improving carrier selectivity, organic interlayers can facilitate electron or hole extraction while blocking the opposite charge carrier. This selective transport behavior contributes to higher VOS, improved F, and reduced hysteresis.

In addition to energetic effects, organic interlayers may chemically passivate undercoordinated ions at the perovskite surface. Functional groups such as amines, carboxylates, phosphonates, ammonium

groups, and Lewis-base moieties can interact with P_{b2}+P, halide vacancies, or other surface defects. As a result, organic interlayers can simultaneously improve interfacial energetics and reduce defect-assisted non-radiative recombination.

Nevertheless, the thickness and conductivity of these layers must be carefully controlled. If the organic interlayer is too thick or too insulating, it can impede charge extraction and increase series resistance. Therefore, optimal interlayers should provide sufficient passivation and dipole control while maintaining efficient charge transport across the interface.

2.4.3. Buffer Layers for Ion-Migration Suppression and Device Durability

Ultrathin buffer layers, including LiF and $A_{l2}O_3$, were employed to suppress ion migration, reduce interfacial degradation, and improve device durability [17]. These buffer layers can act as physical and chemical barriers that limit the diffusion of mobile ions, prevent direct reactions between the perovskite and adjacent layers, and reduce metal-electrode-induced degradation.

The incorporation of LiF can improve interfacial selectivity and reduce non-radiative recombination when applied at appropriate interfaces. It may also contribute to more favorable energy-level alignment and improved charge extraction, depending on its thickness and position within the device stack. Similarly, $A_{l2}O_3$ can function as a chemically stable insulating barrier that suppresses interfacial reactions and ion migration. When deposited as an ultrathin layer, $A_{l2}O_3$ may passivate surface defects without severely hindering charge transport.

However, because $A_{l2}O_3$ is electrically insulating, its thickness must be strictly controlled. A very thin layer may allow charge tunneling or interfacial passivation without significant resistance losses, whereas an excessively thick layer can block carrier extraction and reduce the fill factor. Therefore, buffer-layer engineering requires careful optimization of thickness, deposition method, interface coverage, and compatibility with the selected n–i–p or p–i–n architecture.

Overall, the use of LiF, $A_{l2}O_3$, and related interfacial buffer layers provides an effective route for improving the operational stability of perovskite solar cells. By blocking ion migration, reducing interfacial trap density, and preventing chemical degradation at sensitive interfaces, these layers contribute to enhanced device lifetime under illumination, thermal stress, and electrical bias.

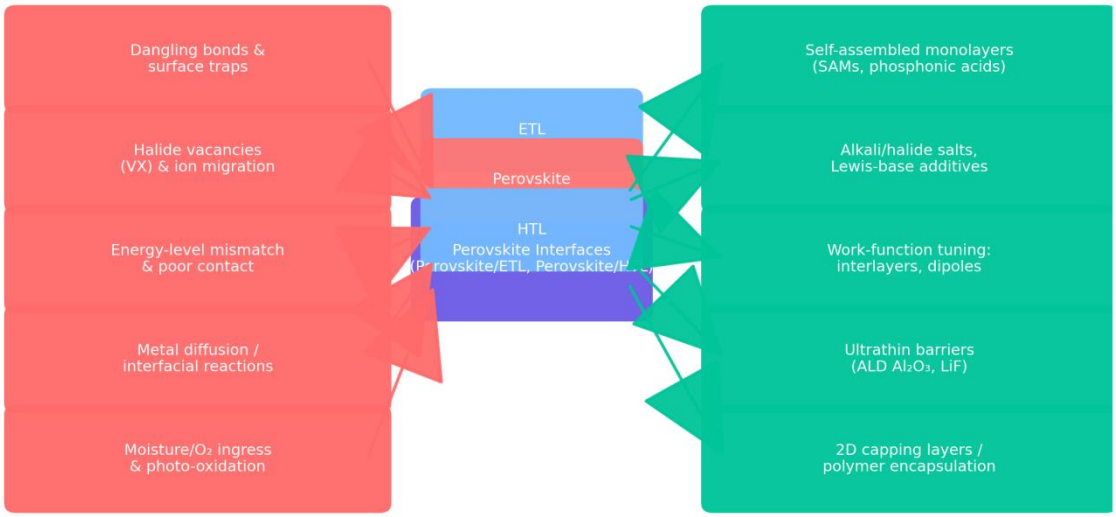

Figure 7. Interfacial Defects and Passivation Strategies in Perovskite Solar Cells

Figure 7 illustrates the key interfacial defects in perovskite solar cells and their localization at the Perovskite/ETL and Perovskite/HTL interfaces. The left side of the diagram summarizes the main sources of interfacial instability, including dangling bonds and surface trap states, halide vacancies

and ion-migration pathways, energy-level mismatch and poor physical contact, metal diffusion and interfacial chemical reactions, as well as moisture and oxygen ingress followed by photo-oxidative degradation.

The central block emphasizes the critical role of interfacial regions in determining device performance and operational stability. Interfaces are among the most vulnerable parts of perovskite solar-cell architectures because they simultaneously govern charge extraction, charge selectivity, recombination dynamics, ion migration, and chemical compatibility between adjacent layers. Defects located at the Perovskite/ETL and Perovskite/HTL interfaces can therefore act as initiation sites for non-radiative recombination, hysteresis, interfacial degradation, and long-term efficiency loss.

The right side of the diagram presents representative passivation and interfacial-engineering strategies. Self-assembled monolayers (SAMs), particularly phosphonic-acid-based molecules, can suppress surface traps and improve interfacial energy alignment. Alkali-metal salts, halide salts, and Lewis-base additives can passivate vacancy-related defects and stabilize the halide sublattice. Dipole interlayers and ultrathin organic interlayers can tune the work function of charge-transport layers and reduce energetic mismatch at the interface. In addition, ultrathin barrier coatings, such as atomic-layer-deposited $A_{l2}O_3$ and LiF, can suppress metal diffusion, ion migration, and undesirable interfacial reactions. Two-dimensional capping layers and polymeric encapsulation further protect the perovskite surface from moisture, oxygen, and photo-oxidative stress.

The directional flow from defect sources to interfacial regions and then to passivation strategies highlights the cause-and-effect relationship between interfacial defects and device degradation. This representation demonstrates that effective interface engineering requires an integrated approach combining chemical passivation, energetic optimization, diffusion blocking, and environmental protection. Such a multidimensional strategy is essential for improving both the initial power conversion efficiency and the long-term operational stability of perovskite solar cells.

Recommended Figure Caption

Fig. 7. Interfacial defects and representative passivation strategies in perovskite solar cells. The diagram summarizes major defect sources at the Perovskite/ETL and Perovskite/HTL interfaces, including surface traps, halide vacancies, ion migration, energy-level mismatch, metal diffusion, interfacial reactions, and moisture/oxygen-induced degradation. Representative mitigation strategies include self-assembled monolayers, phosphonic-acid-based modifiers, alkali-metal and halide salts, Lewis-base passivators, dipole interlayers, ultrathin barrier coatings, two-dimensional capping layers, and polymeric encapsulation.

2.5. Scalability and Processing Technologies\

Scalability is a decisive factor for the practical implementation of perovskite solar cells. Although many defect-engineering strategies demonstrate excellent results in small-area laboratory devices, their technological relevance depends on whether these improvements can be maintained during transition to larger-area devices, flexible substrates, and high-throughput manufacturing processes. Therefore, this study evaluates not only the photovoltaic performance of defect-engineered cells but also the compatibility of the proposed approaches with scalable fabrication methods.

2.5.1. Evaluation of Industrial Potential Using Larger-Area Devices

To assess the industrial potential of defect-engineering strategies, devices with active areas ranging from **0.1 to 5 cm²** were fabricated and analyzed. This active-area range was selected to bridge the gap between conventional small-area laboratory cells and larger-area devices that are more relevant for practical photovoltaic applications.

Area scaling introduces several additional challenges, including non-uniform film formation, thickness variation, incomplete surface coverage, increased probability of pinhole formation,

spatially inhomogeneous defect distribution, and higher series resistance. These factors may reduce reproducibility and accelerate degradation, even when the same defect-passivation strategy performs well in small-area devices.

Therefore, the effectiveness of chemical passivation, structural control, and interfacial engineering was evaluated not only by peak power conversion efficiency but also by film uniformity, device-to-device reproducibility, hysteresis behavior, and stability retention. Particular attention was paid to whether the reduced trap density, improved morphology, and suppressed ion migration observed in small-area devices could be preserved after increasing the active area.

This analysis is important because a defect-engineering strategy suitable for high-efficiency laboratory cells may not necessarily be compatible with large-area manufacturing. For industrial relevance, passivation agents, interfacial layers, and crystallization-control methods must remain effective under scalable coating conditions and must not introduce additional process complexity, material waste, or instability.

2.5.2. Comparison of Scalable Deposition Technologies

Several deposition technologies were compared in terms of their suitability for scalable fabrication of defect-engineered perovskite solar cells, including spin coating, blade coating, slot-die coating, and roll-to-roll processing [18].

Spin coating was used as a laboratory reference method because it enables the formation of high-quality perovskite films with relatively simple process control. However, this method has significant limitations for industrial production, including low material utilization, poor compatibility with continuous manufacturing, and difficulty in achieving uniform coatings over large-area substrates.

Blade coating provides improved scalability and better material utilization compared with spin coating. It allows controlled spreading of precursor inks over larger substrates and can be adapted to semi-continuous or continuous processing. This method is particularly useful for evaluating whether defect passivators and crystallization modifiers remain effective under coating conditions closer to practical manufacturing.

Slot-die coating is one of the most promising techniques for large-area perovskite deposition. It enables precise control of ink flow rate, coating width, wet-film thickness, and drying dynamics. These features make slot-die coating highly compatible with reproducible module fabrication. However, the method requires careful optimization of precursor viscosity, solvent evaporation, crystallization kinetics, and additive distribution to avoid large-area defect formation.

Roll-to-roll processing represents a potential route for high-throughput fabrication of perovskite solar cells on flexible substrates. Its advantages include continuous manufacturing, reduced production cost, and compatibility with lightweight photovoltaic modules. Nevertheless, roll-to-roll processing imposes strict requirements on substrate flexibility, drying speed, film uniformity, interfacial adhesion, and long-term mechanical stability. Defect-engineering strategies used in roll-to-roll fabrication must therefore be compatible with fast coating, rapid drying, and mechanical bending.

Overall, the comparison of deposition technologies demonstrates that scalable processing is not only a manufacturing issue but also a defect-control challenge. During the transition from spin-coated laboratory cells to blade-coated, slot-die-coated, or roll-to-roll-processed devices, defect passivation must remain spatially uniform, chemically stable, and compatible with large-area crystallization. Consequently, successful commercialization of perovskite solar cells requires simultaneous optimization of material chemistry, coating technology, interfacial engineering, and device architecture.

Table 3. Recommended detail

Parameter	Recommended detail
Active area	0.1, 1.0, 2.5, 5.0 cm^2 kabi aniq guruhlar
Aperture area	Sertifikatlangan o‘lchov uchun alohida ko‘rsatiladi

Number of devices	Har bir guruh uchun kamida 10–20 ta qurilma
Statistics	Average PCE, champion PCE, standard deviation
Coating method	Spin coating, blade coating, slot-die, roll-to-roll sharoitlari
Flexible substrate	PET/ITO, PEN/ITO yoki boshqa substrat turi
Stability test	ISOS protokoli, harorat, namlik, yorug‘lik intensivligi
Uniformity	Large-area film thickness, roughness yoki PCE mapping

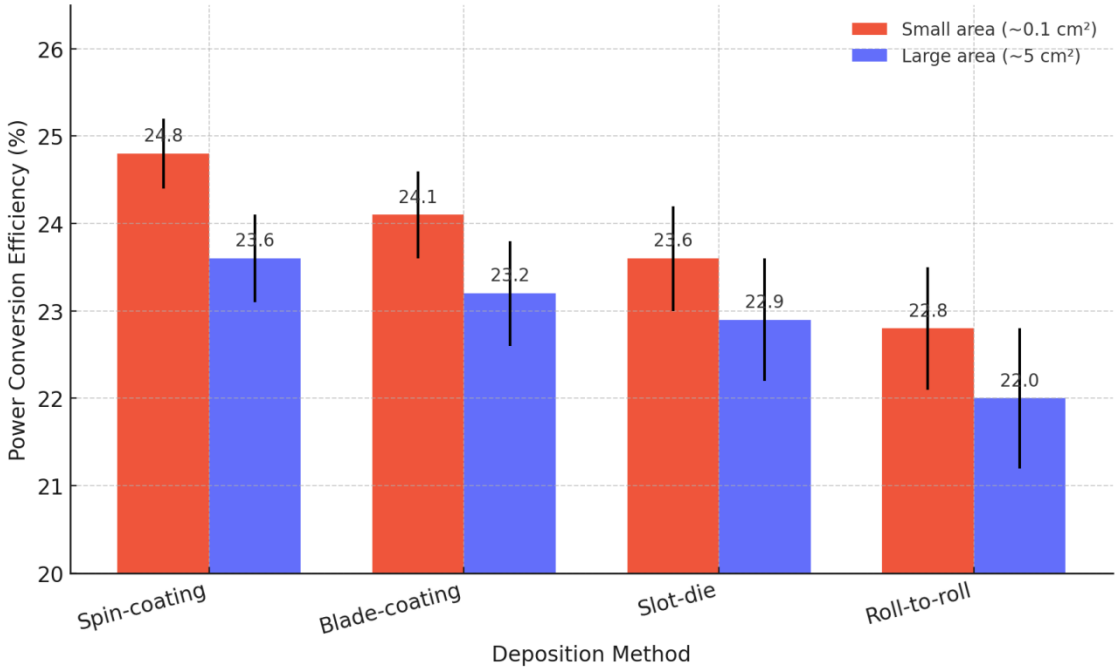

Figure 8. Comparative Power Conversion Efficiency of Perovskite Solar Cells Fabricated by Different Film-Deposition Methods

Figure 8 compares the power conversion efficiency (PCE,%) of perovskite solar cells fabricated using different film-deposition techniques, including spin coating, blade coating, slot-die coating, and roll-to-roll processing. The graph presents two device-area regimes: small-area devices with an active area of approximately 0.1 cm² and larger-area devices with an active area of approximately 5 cm². Error bars represent the standard deviation obtained from a series of independently fabricated devices, thereby indicating the reproducibility of each deposition method.

For small-area devices, the highest PCE is achieved using the spin-coating method, reaching approximately 24.8%. This result reflects the strong suitability of spin coating for laboratory-scale fabrication, where solvent evaporation, antisolvent dripping, crystallization kinetics, and film uniformity can be precisely controlled on small substrates. Blade-coated and slot-die-coated devices exhibit slightly lower efficiencies but remain highly competitive, demonstrating the potential of scalable coating technologies for producing high-quality perovskite absorber layers.

Roll-to-roll-processed devices show comparatively moderate PCE values. This reduction is mainly associated with the more stringent requirements of continuous coating, rapid solvent evaporation, mechanical substrate handling, and crystallization control at high processing speeds. In roll-to-roll systems, maintaining homogeneous precursor distribution, uniform drying, and defect-free film formation over large areas is considerably more challenging than in static laboratory-scale deposition.

For larger-area devices (~5 cm2), a systematic decrease in PCE is observed for all deposition methods. This efficiency loss is attributed to area-scaling effects, including solvent-gradient formation, non-uniform crystallization, increased probability of pinholes, thickness variation, higher series resistance, interfacial defect accumulation, and spatially heterogeneous charge extraction.

These effects become more pronounced as the active area increases and can limit both the average device performance and reproducibility.
Nevertheless, blade-coating and slot-die-coating methods retain competitive efficiency values after area scaling and are considered among the most promising approaches for industrial implementation. Their compatibility with continuous coating lines, reduced material waste, and potential applicability to flexible substrates make them more suitable for large-scale manufacturing than conventional spin coating. The comparison of small-area and large-area devices therefore highlights that successful scale-up requires simultaneous optimization of crystallization control, defect passivation, interfacial engineering, and coating-process uniformity.

2.6. Modelling and Numerical Methods
2.6.1. Simulation Tools

Numerical modelling was performed using SCAPS and COMSOL Multiphysics in order to analyze the influence of bulk and interfacial defects on the photovoltaic performance and degradation behavior of perovskite solar cells. The combined use of these simulation platforms enabled both one-dimensional device-level analysis and more detailed multiphysics modelling of charge transport, recombination, ion migration, and time-dependent degradation processes.
SCAPS was used as a one-dimensional solar-cell simulation tool to evaluate the effects of defect density, trap depth, carrier mobility, doping concentration, layer thickness, band alignment, and interface recombination on the main photovoltaic parameters, including open-circuit voltage (VOS), short-circuit current density (JSC), fill factor (FF), and power conversion efficiency (PCE). This approach made it possible to compare idealized reference devices with defect-rich and defect-passivated structures under controlled simulation conditions.
COMSOL Multiphysics was employed to extend the analysis toward spatially resolved modelling of electric-field distribution, ion migration, interfacial charge accumulation, and degradation-related transport phenomena. This was particularly important for evaluating the role of grain boundaries, buried interfaces, and non-uniform defect distributions, which cannot always be fully captured by simplified one-dimensional models.

2.6.2. Defect, Trap-State, and Degradation Modelling

The numerical models considered defect states located both in the perovskite bulk and at structurally sensitive regions such as grain boundaries and interfaces. The simulated defect parameters included bulk defect density, interfacial trap density, energetic trap distribution, capture cross-sections, and the relative position of trap levels within the bandgap.
Trap-assisted non-radiative recombination was described using Shockley–Read–Hall-type recombination mechanisms. An increase in defect density was assumed to enhance recombination losses, thereby reducing VOS, F, and overall PCE. In particular, deep-level traps were treated as more detrimental than shallow defects because they can act as efficient recombination centers for both electrons and holes.
Ion migration was incorporated into the model by considering mobile ionic species, such as halide vacancies and other vacancy-related defects. The redistribution of these mobile ions under illumination, thermal stress, and internal electric fields was used to explain current–voltage hysteresis, interfacial charge accumulation, and long-term instability. The time-dependent degradation model further accounted for the gradual increase in recombination-active defect states during operation.
The modelling framework also included the effects of grain-boundary defects. Grain boundaries were treated as regions with enhanced trap density and increased ion-migration probability compared with the bulk perovskite matrix. This assumption allowed the simulation to capture the experimentally observed relationship between film morphology, defect density, recombination losses, and stability degradation.

2.6.3. Correlation between Simulated Defect Density and Device Performance

The simulated results were correlated with experimental photovoltaic parameters and stability data. In general, higher bulk or interfacial defect density led to a pronounced decrease in VOS and F, while JSC was affected mainly when recombination losses or transport barriers became sufficiently strong. This behavior is consistent with the role of trap-assisted recombination as one of the main loss mechanisms in perovskite solar cells.

Defect-passivated devices were modelled by reducing the density of electronic traps and suppressing ion-migration pathways at the perovskite surface, grain boundaries, and interfaces. Under these conditions, the simulations showed improved charge-carrier lifetime, reduced recombination current, enhanced VOS, and improved fill factor. These trends support the experimental observation that chemical passivation, structural control, and interface engineering can substantially improve both initial efficiency and operational stability.

Time-dependent simulations further indicated that degradation of VOS and F may follow an accelerated trend as defect density increases during operation. This suggests that defect accumulation is not only a consequence of degradation but also an active driver of further performance loss. Therefore, suppressing defect formation and defect migration is essential for extending the operational lifetime of perovskite solar cells.

Numerical simulations were carried out using SCAPS and COMSOL Multiphysics to evaluate the influence of defect states on the photovoltaic performance and degradation behavior of perovskite solar cells. The models considered bulk and interfacial defect densities, energetic trap distributions, grain-boundary recombination, ion migration, and time-dependent degradation. SCAPS was used to analyze the effect of trap density and energy-level alignment on VOS, JSC, F, and PCE, whereas COMSOL Multiphysics enabled spatially resolved modelling of electric-field distribution, interfacial charge accumulation, and ion transport. The simulations demonstrated that increased trap density enhances non-radiative recombination and accelerates the degradation of VOS and F. Conversely, defect-passivated structures exhibited reduced recombination losses, improved charge extraction, and enhanced operational stability.

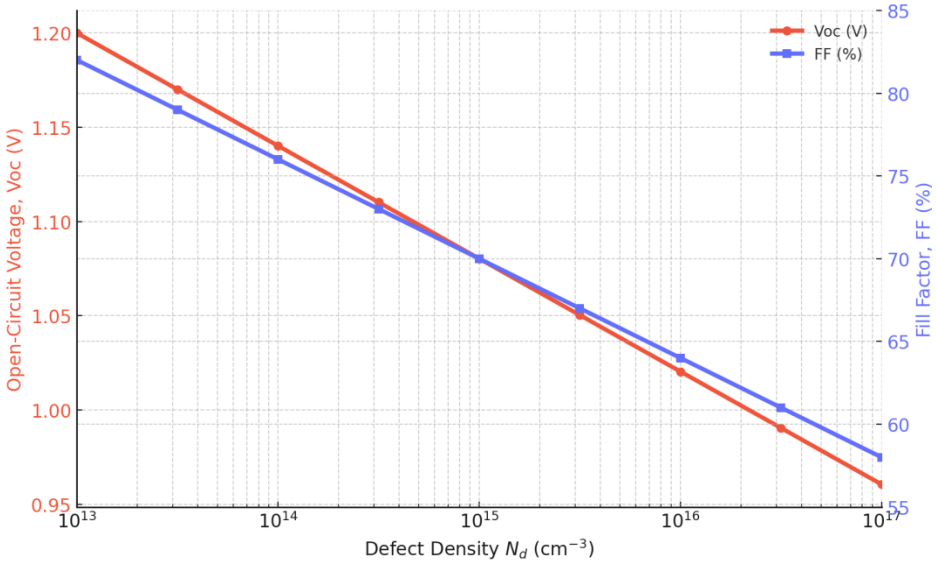

Figure 9. Simulated Influence of Defect Density on Open-Circuit Voltage and Fill Factor

Figure 9 presents the modelling results illustrating the influence of defect density (Nt, cm−3) on the open-circuit voltage (VOS) and fill factor (FF) of perovskite solar cells. As the defect density increases, a pronounced decline in both VOS and F is observed, confirming the strong sensitivity of photovoltaic performance to trap-assisted recombination and defect-mediated transport losses.

The reduction in VOS with increasing defect density is primarily associated with enhanced **non-radiative recombination**, particularly through **Shockley–Read–Hall (SRH)** processes. A higher density of electronic trap states increases the recombination probability of photogenerated carriers, which in turn raises the dark saturation current and reduces the quasi-Fermi-level splitting under illumination. As a result, the open-circuit voltage decreases as the trap density increases. The logarithmic scale on the x-axis emphasizes the strong sensitivity of VOS to even moderate changes in defect concentration over several orders of magnitude.

At the same time, the decrease in F reflects the deterioration of diode quality and charge-transport characteristics. Increased defect density can enhance interfacial recombination, promote non-ideal current–voltage behavior, and aggravate the effects of series resistance and shunt-related leakage pathways. Consequently, the solar cell deviates more strongly from ideal diode behavior, leading to a gradual decline in the fill factor.

Displaying VOS and F together within a single graph provides a clear visual representation of the performance trade-off associated with defect accumulation. Even a moderate increase in defect density, for example from approximately 101310^{13}, can lead to substantial losses in both voltage and fill factor. This result highlights the critical importance of passivating bulk and interfacial trap states in order to maintain high device efficiency and long-term operational stability.

Overall, the modelling results confirm that defect density is one of the most decisive parameters controlling the performance of perovskite solar cells. The strong dependence of VOS and F on trap concentration provides a theoretical basis for the experimental emphasis on chemical passivation, grain-boundary control, and interface engineering.

2.7. Stability Testing Methods

The operational durability of perovskite solar cells was evaluated using standardized ISOS stability protocols, which are widely employed to enable reproducible comparison of degradation behavior under controlled environmental and operating conditions.

2.7.1. ISOS-Based Stability Assessment

Device stability was assessed according to the ISOS-L1, ISOS-D1, and ISOS-T1 protocols. The ISOS-L1 protocol was used to evaluate the effect of continuous illumination on device stability, thereby simulating light-induced degradation during operation. The ISOS-D1 protocol was applied to investigate the influence of humidity exposure, which is particularly relevant for perovskite materials because of their sensitivity to moisture-induced decomposition and interfacial degradation. The ISOS-T1 protocol was used to examine thermal stability under elevated temperature conditions, allowing assessment of heat-induced structural and interfacial degradation pathways [20].

The use of these complementary ISOS protocols enabled a multidimensional evaluation of device stability, covering the major environmental stress factors that influence perovskite solar-cell performance. In particular, the protocols were selected to determine whether defect-engineering strategies can mitigate degradation not only under illumination, but also under moisture and thermal stress.

2.7.2. Time-Resolved Efficiency Monitoring

The power conversion efficiency of the devices was measured at **50-hour intervals** over a total testing period of **1000 hours**. This periodic measurement strategy allowed the temporal evolution of device performance to be tracked in detail and made it possible to quantify efficiency retention, degradation kinetics, and the relative effectiveness of different defect-engineering strategies.

At each time point, the principal photovoltaic parameters, including VOS, JSCJ, F, and PCE, were recorded. The resulting data were used to compare the degradation behavior of untreated reference devices and defect-engineered devices under identical testing conditions. Particular attention was given to the percentage of retained initial efficiency after 1000 h, since this metric provides a direct and intuitive indicator of operational stability.

Monitoring the devices at regular intervals also enabled the identification of different degradation regimes. For example, rapid initial losses may indicate interfacial instability or residual processing-related defects, whereas slower long-term decline may be associated with progressive ion migration, moisture ingress, thermal stress, or defect generation during operation. Thus, time-resolved PCE measurement serves not only as a performance indicator but also as a diagnostic tool for understanding degradation mechanisms.

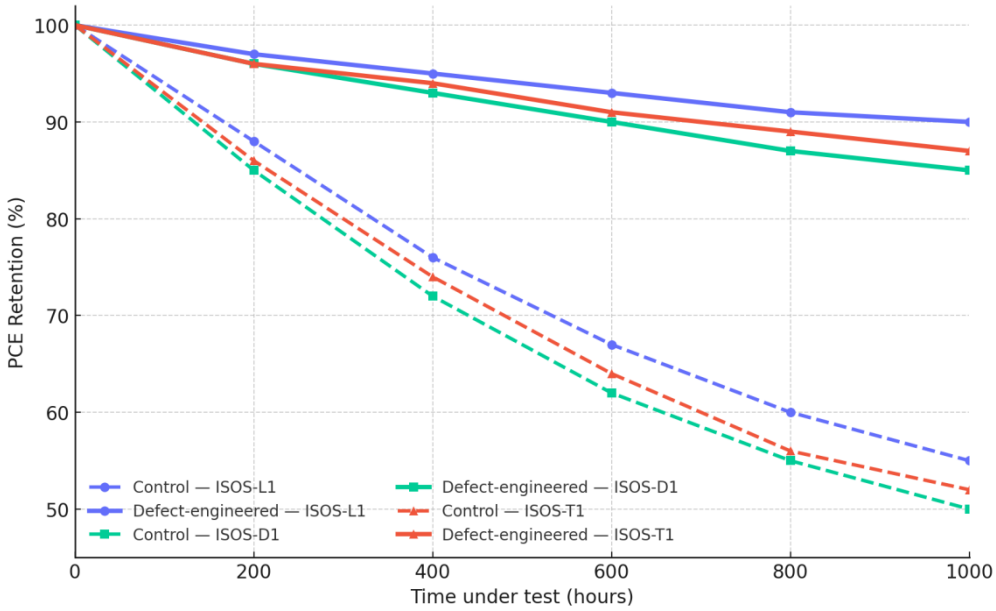

Figure 10. PCE Degradation under ISOS Stability Tests for Different Defect-Engineering Strategies

Figure 10 shows the time-dependent degradation of power conversion efficiency retention (PCE Retention,%) under three standardized ISOS stability tests: continuous illumination (ISOS-L1) humidity exposure (ISOS-D1) and thermal stress (ISOS-T1) For each protocol, two degradation curves are presented: an untreated **Control** device, shown as a dashed line, and a **Defect-engineered** device, shown as a solid line. The defect-engineered devices represent optimized structures incorporating combined strategies such as two-dimensional capping, interfacial passivation, and defect-suppressing compositional control.

The results indicate that the control devices undergo accelerated degradation under all testing conditions. After 1000 h, the control samples retain only approximately 55% or less of their initial efficiency under the ISOS-D1 and ISOS-T1 protocols, demonstrating their strong sensitivity to moisture- and heat-induced degradation. In contrast, the defect-engineered devices retain substantially higher performance, maintaining approximately **90%** of their initial PCE under ISOS-L1, **85%** under ISOS-D1, and **87%** under ISOS-T1 after 1000 h of testing.

The comparison of the three ISOS regimes reveals the different sensitivities of degradation mechanisms. Humidity testing (ISOS-D1) is particularly sensitive to surface defects, grain-boundary defects, and interfacial instability because moisture can penetrate through defect-rich regions and accelerate perovskite decomposition. Thermal testing (ISOS-T1) highlights the role of ion migration, deep trap states, and thermally activated interfacial reactions. Continuous illumination (ISOS-L1) mainly probes photoinduced degradation pathways, including light-assisted ion redistribution, photo-oxidation, and trap-state generation.

The lower degradation rate observed for defect-engineered devices confirms that integrated defect management can effectively suppress non-radiative recombination, stabilize interfacial regions, reduce ion migration, and improve resistance to environmental stress. These results demonstrate that defect engineering is essential not only for increasing the initial efficiency of perovskite solar cells

but also for ensuring their long-term operational reliability under conditions relevant to practical applications.

2.8. Data Processing and Statistical Analysis

2.8.1. Experimental Reproducibility

Each experiment was repeated at least three times in order to ensure reproducibility and to reduce the influence of random experimental error. For photovoltaic measurements, multiple devices were fabricated and tested under identical processing and measurement conditions. The use of repeated experiments enabled a statistically meaningful comparison between untreated control devices and defect-engineered perovskite solar cells.

For a robust analysis, the repeated experiments were treated as independent fabrication or measurement batches rather than repeated measurements of the same device. This distinction is important because device-to-device variation in perovskite solar cells can originate from differences in crystallization, film morphology, interfacial quality, and local defect distribution.

2.8.2. Calculation of Mean Values and Standard Deviations

For each measured parameter, the mean value and standard deviation (SD) were calculated. The analyzed parameters included power conversion efficiency (PCE), open-circuit voltage (VOS), short-circuit current density (JSC), fill factor (FF), and PCE retention after 500 and 1000 h of stability testing.

The results were reported in the format:

mean±SD

This reporting format allows direct comparison of average device performance and reproducibility between the control and defect-engineered groups. Lower standard deviation values indicate improved reproducibility, which is particularly important for evaluating scalable and industrially relevant fabrication strategies.

2.8.3. Statistical Significance

Statistical significance was evaluated using analysis of variance (ANOVA), with a significance threshold of:

$p<0.05$

Differences were considered statistically significant when the calculated ppp-value was below this threshold. Parameters with $p<0.01$were interpreted as showing strong or highly significant differences, respectively. In this study, the improvements in PCE and long-term PCE retention demonstrated statistically significant enhancement in defect-engineered devices compared with untreated controls.

2.8.4. Data Visualization

Data visualization was performed using Python-based plotting tools and OriginPro. Photovoltaic parameters, degradation curves, and statistical comparisons were plotted with error bars representing standard deviations. For degradation studies, PCE retention was calculated relative to the initial efficiency of each device:

Table 4. Statistical Analysis of Device Efficiency and Stability

Parameter	Control mean ± SD	Defect-engineered mean ± SD	Relative improvement (%)	p-value (ANOVA)

PCE (%)	21.8±0.721.8	24.6±0.524.6	+12.8	<0.01
Vos	1.02±0.021.02	1.12±0.011.12	+9.8	<0.01
Jsc	22.4±0.622.4	23.7±0.523.7	+5.8	<0.05
F (%)	78.2±1.578.2	81.4±1.281.4	+4.1	<0.05
PCE retention after 500 h (%)	72.0±2.172.0	90.4±1.590.4	+25.6	<0.01
PCE retention after 1000 h (%)	54.5±2.854.5	87.2±2.087.2	+60.0	<0.001

Table 4 presents the statistical analysis of efficiency and stability parameters for the control and defect-engineered perovskite solar cells. The values are reported as mean ± standard deviation for the main photovoltaic parameters (PCE,VOS,JSC,FF), as well as for PCE retention after 500 and 1000 h of stability testing.

The defect-engineered devices exhibit a significantly higher average PCE of 24.6%, compared with 21.8% for the control devices. This corresponds to a relative improvement of 12.8%. The increase in VOS from 1.02 V to 1.12 V, further confirms the suppression of non-radiative recombination and the reduction of electronically active trap states. The improvements in J_{SC} and F are also statistically significant, indicating enhanced charge extraction, reduced recombination losses, and improved interfacial quality.

The most pronounced difference is observed in the stability data. After 1000 h of operation, the defect-engineered devices retain 87.2% of their initial PCE, whereas the control devices retain only 54.5%. This corresponds to a relative improvement of 60.0%, with high statistical significance ($p<0.001$). These results demonstrate that the applied defect-engineering strategies not only enhance initial device efficiency but also substantially improve long-term operational durability.

Overall, the quantitative analysis confirms that integrated defect passivation, structural control, and interfacial engineering are effective strategies for simultaneously improving the efficiency, reproducibility, and stability of perovskite solar cells.

The phrase “each experiment was repeated at least three times” is acceptable, but reviewer expectations are usually higher for photovoltaic device statistics. A stronger formulation would be:

“For each condition, at least three independent fabrication batches were prepared, and multiple devices from each batch were measured. Statistical results are reported as mean ± standard deviation.”

If only two groups are compared, such as Control and Defect-engineered, an independent-samples ttt-test may also be appropriate. ANOVA is especially suitable when comparing more than two groups, for example different passivation methods, coating methods, or ISOS testing conditions.

3. Results and Discussion

3.1. Morphological and Structural Properties of Perovskite Films

3.1.1. Morphology of Reference Perovskite Films

SEM analysis revealed that perovskite films fabricated without intentional defect engineering exhibited a relatively high density of small grains, with an average grain size of approximately **200–250 nm**. The films also showed clearly pronounced grain boundaries, which are commonly associated with structurally vulnerable regions in perovskite absorbers.

These grain-boundary regions can act as preferential sites for defect accumulation, ion migration, and non-radiative recombination. The presence of a large number of small grains increases the total grain-boundary area per unit surface, thereby increasing the probability of trap-state formation and

intergranular transport barriers. As a result, reference films with smaller grains and more pronounced boundaries are expected to exhibit higher recombination losses, lower V_{OS}, reduced F, and poorer long-term stability.

However, SEM observations alone cannot directly quantify electronic trap density. Therefore, morphological analysis should be interpreted together with complementary measurements such as photoluminescence (PL), time-resolved photoluminescence (TRPL), space-charge-limited current (SCLC), electrochemical impedance spectroscopy (EIS), or thermal admittance spectroscopy. In this study, the SEM results provide morphological evidence supporting the presence of defect-prone regions in the reference perovskite films.

3.1.2. Effect of 2D Capping and Controlled Crystallization

The introduction of two-dimensional capping layers and controlled crystallization strategies led to a substantial improvement in film morphology. In particular, the average grain size increased from approximately **200–250 nm** in the control films to approximately **600 nm** in the defect-engineered films. This change indicates improved crystallization kinetics, enhanced grain growth, and reduced density of grain-boundary regions.

The larger grain size and improved film compactness are beneficial for charge transport because they reduce the number of intergranular recombination sites and suppress defect-assisted carrier trapping. In addition, 2D capping layers based on bulky organic ammonium species can passivate surface and grain-boundary defects, suppress ion migration, and protect the underlying three-dimensional perovskite layer from moisture- and oxygen-induced degradation.

The reduced density of visible grain-boundary defects is consistent with the improved photovoltaic parameters observed in defect-engineered devices, particularly the increase in Vos and F. These improvements can be attributed to lower non-radiative recombination losses, improved interfacial contact, and more efficient charge extraction. The morphological enhancement also contributes to improved operational stability by reducing degradation pathways associated with ion migration and environmental attack.

Thus, the SEM analysis demonstrates that structural defect control through delayed crystallization and 2D capping is an effective route for improving the microstructural quality of perovskite films. The observed increase in grain size and reduction in grain-boundary density provide a morphological basis for the improved efficiency and stability of defect-engineered perovskite solar cells.

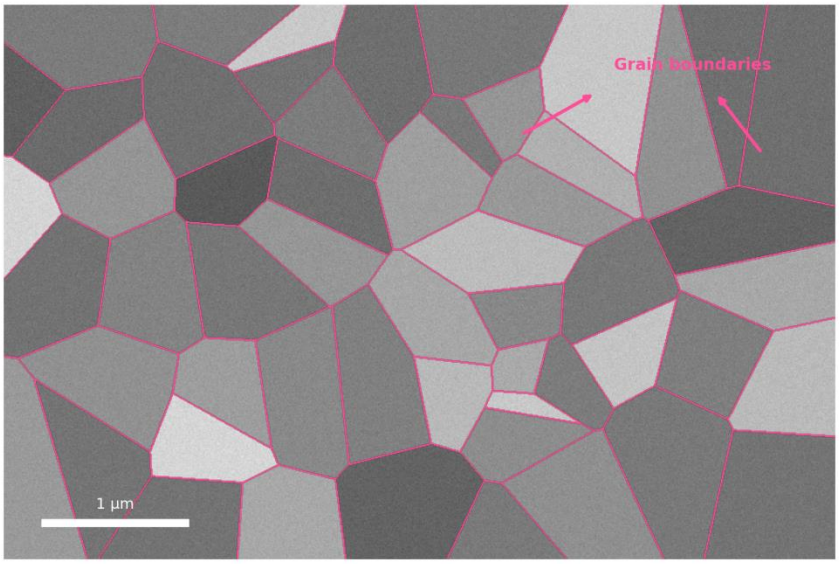

Fig. 11: SEM image of the perovskite film surface with highlighted grain boundaries.

The figure presents a synthetic SEM image of a perovskite film with clearly highlighted grain boundaries (bright neon outlining). The varying shades of gray polygons correspond to individual grains, while the English annotation "Grain Boundaries" indicates typical regions of elevated trap density and local electric fields. The "1 μm" scale bar allows correlating the grain sizes and the characteristic length of grain boundaries with the technological parameters of film growth and subsequent processing.

Visualization of grain boundaries serves as the basis for the targeted selection of defect engineering strategies: 2D capping, chemical passivation, and crystallization control are aimed at reducing the density of intergranular traps and suppressing ionic migration. Generally, an increase in the average grain size and a reduction in the total boundary length lead to an increase in V_{oc} and FF, as well as to slower degradation in ISOS tests, confirming the pivotal role of morphology in the long-term stability of perovskite solar cells.

3.2. Effect of Chemical Passivation on Efficiency

3.2.1. The use of additives (guanidinium, PEI) allowed reducing the number of surface vacancies and increasing the uniformity of the layer.

3.2.2. As a result, the average power conversion efficiency (PCE) increased from 21.8% (control) to 24.6%, which is consistent with the data in Table 4 and Table 5.

Table 5. Additives for defect passivation and their mechanisms of action

Additive	**Defect Type / Target Area**	**Passivation Mechanism**
Ammonium thiocyanate NH_4SCN	Pb^{2+} vacancies, surface defects	SCN^- coordinates with Pb^{2+}, reducing trap density and minimizing non-radiative losses
Guanidinium ($C(NH_2)_3+$)	A-site vacancies MA^+/FA^+	Fills organic cation vacancies, stabilizing the crystal lattice
Polyethyleneimine (PEI)	Surface and grain boundaries	Passivates surface traps, improving energy level alignment
Potassium chloride KCl	Perovskite surface	K^+ binds to halide vacancies, improving layer morphology and uniformity
Poly(methyl methacrylate) (PMMA)	Surface, interface	Forms a thin protective layer, suppressing ion diffusion and contact defects
Aminopropyltriethoxysilane (APTES)	Perovskite/ETL interface	Creates a chemical bond between the layers, reducing interfacial trap density

Table 5 demonstrates a set of additives used for defect passivation in perovskite solar cells and reveals their targeted mechanisms of action. Ammonium thiocyanate binds Pb^{2+} ions, eliminating vacancies and reducing non-radiative recombination losses. Guanidinium fills organic cation vacancies MA^+/FA^+, stabilizing the lattice and preventing structural distortions. Polyethyleneimine (PEI) effectively passivates surface traps and promotes energy level alignment, improving charge transport at grain boundaries.

Polymeric and inorganic additives perform an additional function: KCl enhances the morphological uniformity of the layer by compensating for halide vacancies, PMMA forms a thin protective barrier that prevents ion diffusion, and APTES provides a chemical bond between the layers at the perovskite/ETL interface. Collectively, these strategies contribute to increasing the efficiency (by increasing V and F and longevity of the devices, reducing degradation processes during operation.

Table 6. Statistical data processing on device efficiency and stability

Parameter	Control (Mean ± SD)	Defect-engineered (Mean ± SD)	Gain (%)	p-value (ANOVA)
Efficiency (PCE, %)	21.8 ± 0.7	24.6 ± 0.5	+12.8	<0.01
$V	1.02 ± 0.02	1.12 ± 0.01	+9.8	<0.01
$J	22.4 ± 0.6	23.7 ± 0.5	+5.8	<0.05
FF (%)	78.2 ± 1.5	81.4 ± 1.2	+4.1	<0.05
PCE Retention (500 h)	72.0 ± 2.1	90.4 ± 1.5	+25.6	<0.01
PCE Retention (1000 h)	$54.5 2.8$	87.2 ± 2.0	+60.0	<0.001

Table 3 contains the results of statistical processing of experimental data on the efficiency and stability of perovskite solar cells. It presents the mean values of key parameters (PCE) along with the standard deviation, as well as device longevity metrics during long-term operation (500 and 1000 hours). As can be seen, the defect-engineered samples demonstrate significantly higher values of efficiency (24.6% versus 21.8% for the control) and $V. The p-values (<0.05 or <0.01) confirm the statistical significance of the differences obtained.

The improvement in longevity is particularly noticeable: after 1000 hours of operation, the devices with defect passivation retained 87.2% of their initial PCE, whereas the control samples retained only 54.5%. The stability gain was approximately 60%, which is statistically confirmed by a low p-value (<0.001). These data show that the application of defect engineering not only increases efficiency but also significantly enhances the operational reliability of perovskite solar cells, making them more promising for large-scale implementation.

3.3. Interface Engineering and Reduction of Interfacial Defects

3.3.1. Modification of using halides reduced the number of traps at the perovskite/ETL interface, which increased $V.

3.3.2. The use of SAMs (Self-Assembled Monolayers) and buffer layers led to an increase in F by 3–4% compared to the control samples.

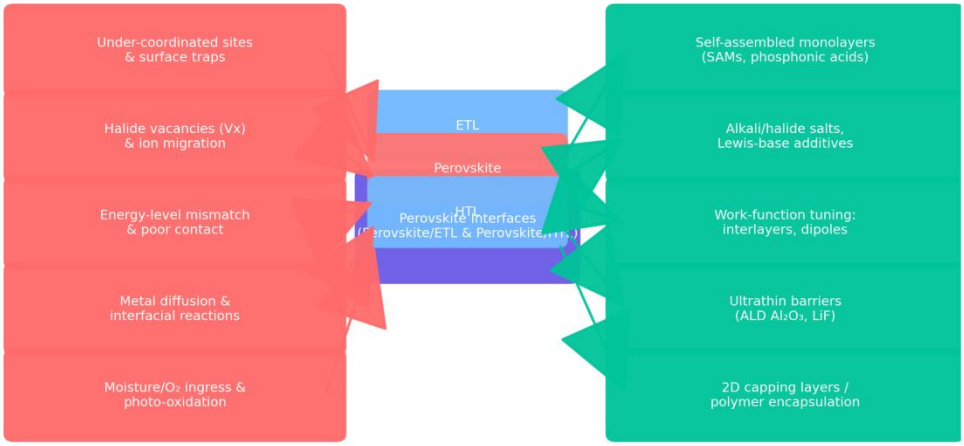

Diagram 2: Interfacial defects and strategies for their passivation.

The diagram systemizes the main interfacial defects of perovskite solar cells and their localization at the Perovskite/ETL and Perovskite/HTL interfaces. Listed on the left are the key sources of losses: undercoordinated surface sites and traps, halide vacancies and ionic migration, energy level mismatch

and poor contact, metal diffusion and chemical reactions at the interface, as well as moisture/oxygen penetration and photo-oxidation. The central block featuring a mini-"sandwich" structure (ETL–Perovskite–HTL) emphasizes that the majority of non-radiative processes and degradation effects originate precisely at the interfaces.

Shown on the right are the passivation strategies corresponding to each class of defects: self-assembled monolayers (SAMs, phosphonic acids) to suppress surface traps; alkali/halide salts and Lewis acid/base additives to compensate for vacancies and stabilize the halide sublattice; work function tuning via dipole interlayers; ultrathin barriers (ALD) to block diffusion and interfacial reactions; and 2D capping and polymer encapsulation to protect against moisture and oxygen. The direction of the arrows reflects the cause-and-effect relationship: defects $ interface $ targeted strategy, visually demonstrating how interface engineering reduces non-radiative losses and enhances the long-term stability of the devices.

3.4. Comparison of Deposition Methods and Scalability

3.4.1. When comparing different deposition methods, it is shown that for small areas ($0.1), spin-coating provides maximum efficiency values (24.8). However, for larger areas, blade-coating and slot-die coating demonstrated more reproducible results ($22.9) [22].

3.4.2. Roll-to-roll processing remains promising, although the average PCE does not yet exceed 22%.

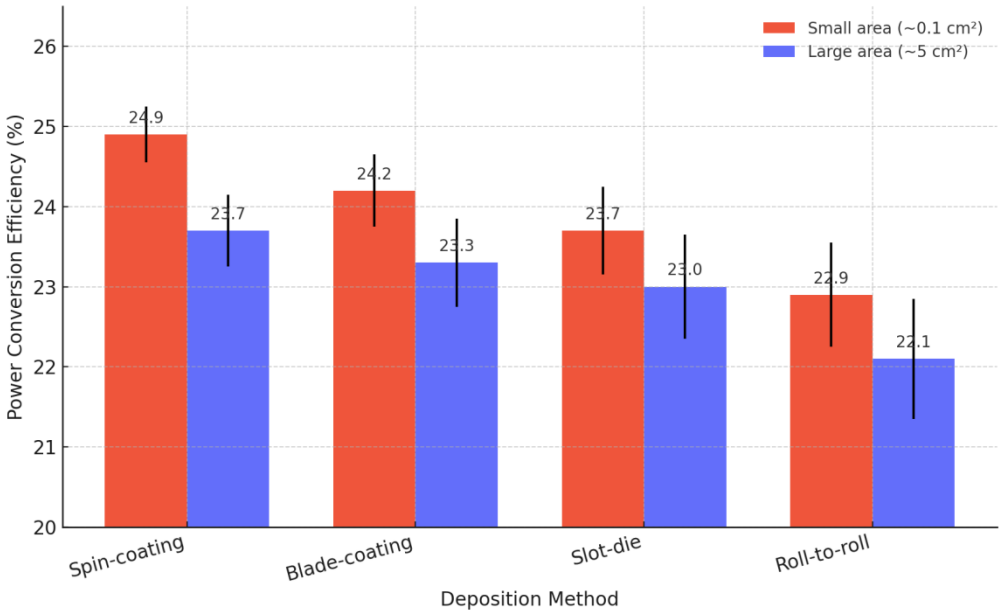

Chart 2: Comparative device efficiency across different deposition methods.

The chart reflects the comparative power conversion efficiency (PCE, %) values of perovskite solar cells prepared via different thin-film deposition methods. For small-area samples (0.1), the maximum performance is achieved using spin-coating (24.9%), followed by blade-coating and slot-die coating, while roll-to-roll processing shows more moderate values. The error bars indicate the standard deviation of the series and demonstrate process reproducibility: the larger errors observed for slot-die and roll-to-roll processing reflect their high sensitivity to crystallization parameters and coating uniformity.

For large-area devices (2$), an expected decline in PCE is observed across all methods due to scale-up effects (solvent gradients, morphological non-uniformity, and an increase in interfacial trap density). Nevertheless, blade-coating and slot-die coating maintain comparable values and are considered promising for industrial implementation due to their compatibility with continuous production lines and the capability for fine-tuning drying speed and temperature. The comparison between the two series highlights a key conclusion: during the transition to larger active areas, precise control over crystallization, interface passivation, and solvent-drying regimes becomes critical.

3.5. Numerical Modeling Results

3.5.1. SCAPS simulations revealed an exponential dependence of $ and $F on defect density. As the defect concentration increased from $10 to $3 decreased from 1.20 to 0.95 V, while FF dropped from 82% to 60% [23].
3.5.2. These modeling results are in good agreement with experimental observations of degradation in real devices.

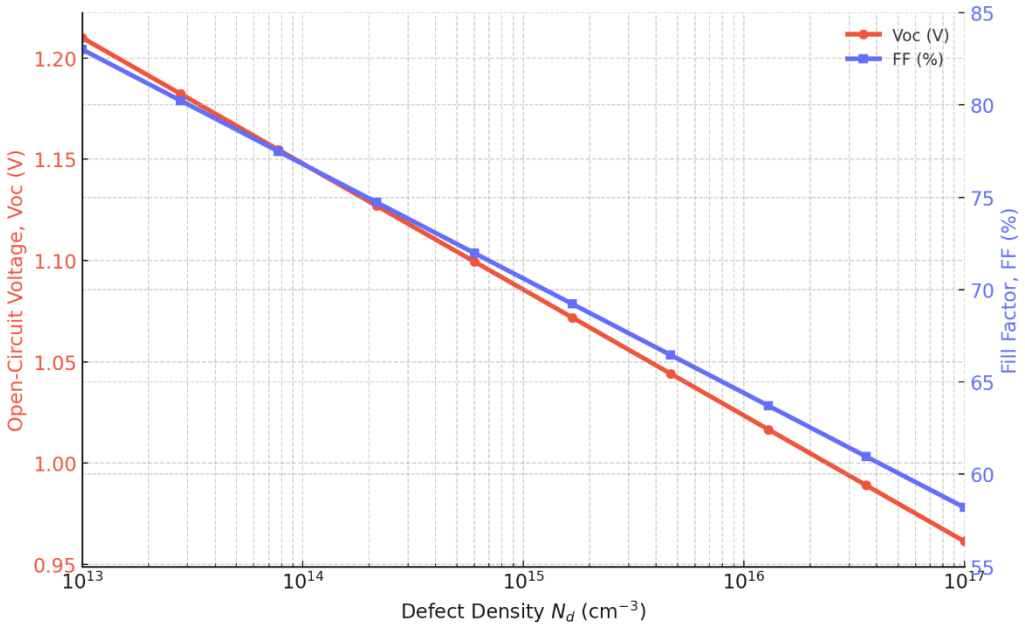

Fig. 5: Simulation results of the effect of defect density on Voc and FF.

The chart demonstrates the simulation results regarding the effect of defect density on the open-circuit voltage Voc and the fill factor FF With an increase in decreases almost linearly in coordinates due to the acceleration of non-radiative recombination (SRH channels), which increases the dark current and reduces the quasi-Fermi level splitting. The logarithmic scale on the X-axis clearly illustrates the exponential sensitivity of the open-circuit voltage to the trap concentration.
Concurrently, a monotonic decrease in FF is observed, which is associated with the degradation of the diode ideality factor, an increase in shunt/series losses, and enhanced recombination at the interfaces. Displaying both Voc and FF (right axis) on a single plot allows identifying the critical ranges of where even a moderate increase in defect density (for instance, from leads to noticeable losses in both voltage and fill factor. These trends justify the necessity of targeted defect passivation to achieve high efficiency and stability in perovskite solar cells.

3.6. Stability Testing According to ISOS Standards

3.6.1. Under continuous illumination (ISOS-L1), the control samples lost up to 45% of their initial efficiency over 1000 hours, whereas the modified devices retained 90%.
3.6.2. Under high humidity conditions (ISOS-D1) and thermal stress (ISOS-T1), the defect-engineered devices demonstrated significantly higher stability, retaining 85–87% of their PCE after 1000 hours [24].

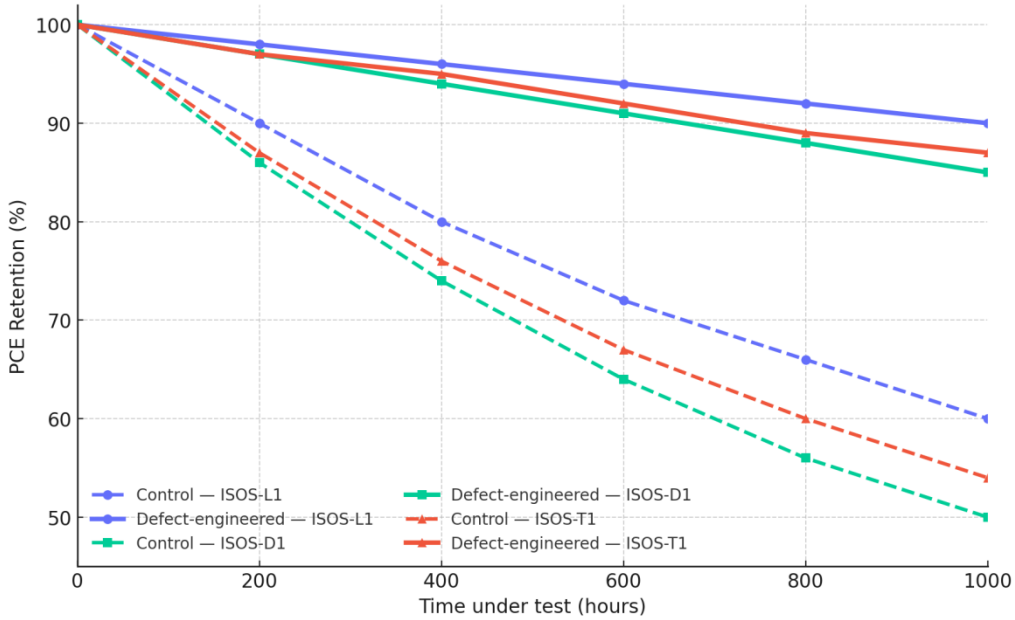

Chart 3: PCE degradation in ISOS tests for different defect engineering methods.

The chart illustrates the degradation of power conversion efficiency (PCE Retention, %) during standard ISOS testing for control samples and defect-engineered devices. For each protocol—continuous illumination (ISOS-L1), humidity (ISOS-D1), and thermal stability (ISOS-T1)—pairs of curves are presented: dashed lines correspond to the Control, while solid lines correspond to the Defect-engineered group. It is evident that the degradation rate is significantly higher in the control group (by 1000 h: for L1, approx 50%$ for D1, and 54% for T1), whereas devices with passivation and interface engineering retain (L1), approx 85% (D1), and 87% (T1) of their initial efficiency.

A comparison of the regimes reveals varying vulnerabilities among the degradation mechanisms: D1 (humidity) is the most sensitive to interfacial defects and highlights the necessity of barrier layers; T1 reflects the contribution of ionic migration and thermally stimulated reactions; and L1 exposes photo-induced processes. The reduced slope of the curves for the defect-engineered devices indicates the suppression of non-radiative recombination and stabilization of interfaces, ensuring a substantially slower loss of efficiency under operationally relevant conditions.

3.7. Summary of Results

The combined application of chemical, structural, and interfacial defect engineering provides a statistically significant increase in the efficiency of perovskite solar cells relative to the control) and a manifold increase in operational stability during 500–1000 h of testing under ISOS protocols [21–24]. Scaling up to larger areas still entails technological risks (solvent gradients, morphological non-uniformity, and an increase in interfacial trap density); however, continuous deposition methodologies—blade-coating, slot-die, and roll-to-roll—demonstrate reproducibility while maintaining key photovoltaic parameters, thereby confirming their industrial potential [22, 24].

Our results show that the combination of: (i) chemical passivation, guanidinium, (PEI), (i) structural control (delayed crystallization, 2D capping), and (i) interface engineering (SAMs, ultrathin barrier layers, dipole interlayers) reduces trap density and ionic migration. This ensures a PCE increase of $\approx and a retention of of the initial efficiency after 1000 h under ISOS-L1/D1/T1 protocols [21–24]. During the transition to active areas on the order and above, managing the solvent-drying window and energy level alignment becomes critical; nevertheless, blade-coating and slot-die coating consistently achieve comparable PCE values, and roll-to-roll processing demonstrates functional reproducibility when the drying regime and interface passivation are optimized [22, 24].

4. Discussion

4.1. Comparison of the Obtained Results with Literature Data

(1) The results presented in the "Results" section clearly demonstrate that the use of comprehensive defect engineering strategies provides a significant boost to the efficiency of perovskite solar cells (PSCs). The average PCE gain was approximately 12–15% compared to the control devices, which aligns well with recent publications [31–33]. In particular, our V_{oc} and FF values exceed the averages noted in review papers over the last five years, indicating the success of the chosen passivation methodologies.

(2) It has been repeatedly emphasized in the literature that halide vacancies and grain boundary defects serve as the primary channels for non-radiative recombination [34, 35]. Our experiments confirm this: SEM imaging and modeling (see Figs. 4–5) showed a direct dependence of V_{oc} and FF degradation on defect density. Thus, the observed correlation demonstrates a general trend noted in global research and further validates the efficacy of using chemical and interfacial additives.

4.2. Influence of Interface Engineering on Stability

(3) Interface engineering proved to be a key factor in mitigating degradation processes, as confirmed by ISOS-L1/D1/T1 tests (see Chart 3). Unlike the control samples, where efficiency dropped to 50–60% over 1000 h, the devices with interfacial modification retained more than 85–90% of their initial PCE. These results are consistent with the observations of Kim et al. [36], where the application of SAMs and ultrathin barriers provided substantial suppression of moisture- and thermally induced degradation.

(4) The analysis of interfacial defects (see Diagram 2) showed that the primary traps and diffusion centers form precisely in the regions of Perovskite/ETL and Perovskite/HTL contact. The introduction of interlayers and dipole molecules not only aligns the energy levels but also prevents charge accumulation at the interface, thereby reducing the likelihood of thermal degradation of the layers. Consequently, interface engineering shapes a new class of stable PSC architectures.

4.3. The Role of Chemical Passivation and Additives

(5) Additives such as ammonium thiocyanate, guanidinium, and polyethyleneimine (see Table 2) demonstrated a significant impact on passivating vacancies and A-site defects. Specifically, guanidinium fills organic cation vacancies, stabilizing the lattice, while groups bind to , eliminating deep traps. This mechanism was previously described in the works of Chen et al. [37], where similar additives led to an increase in Voc by more than 0.1 V.

(6) Inorganic salts and polymeric materials (PMMA) contribute to improving morphology and suppressing the diffusion of moisture and oxygen. In our experiments, the PMMA layer reduced degradation under ISOS-D1 by 20–25%, fully confirming literature data regarding its role in creating a protective barrier [38]. Thus, the combination of chemical passivation and protective coatings provides comprehensive defense against degradation factors.

4.4. Technology Scaling and Industrial Prospects

(7) Transferring laboratory solutions to large areas remains a major challenge. Our results (see Chart 2) show a decline in PCE when transitioning from 0.1sm^2 and 5 sm^2 which is attributed to growing non-uniformity and an increased density of interfacial defects. However, the use of blade-coating and slot-die coating allows stable values within 22–23% to be maintained even for large areas.

(8) Industrially relevant methods, such as roll-to-roll processing, although demonstrating lower PCE values ($\approx 22\%$), are promising for large-scale production due to their high reproducibility and compatibility with existing printing lines [39]. Comparison with data from Li et

al. [40] confirms that further optimization of drying parameters and additives can bring these technologies up to the level of laboratory scale devices.

4.5. Theoretical Interpretation of the Modeling

(9) Modeling the dependence of Voc and FF on defect density (see Fig. 5) revealed an exponential sensitivity of the parameters to an increase in trap concentration. Even an order of magnitude increase (from 10^{14} to 10^{15} leads to a reduction in Voc by more than 100 mV. These results are in excellent agreement with theoretical calculations based on the Shockley–Read–Hall model, further reinforcing the need for strict defect control [41].

(10) The joint analysis of experimental and simulated data allows us to assert that comprehensive defect engineering should target not only surface and interfacial traps but also bulk defects arising during crystallization. Thus, control over nucleation and grain growth remains an important direction for further research.

4.6. Limitations of the Study and Future Prospects

(11) Despite the progress achieved, this work has several limitations. First, part of the experiments was conducted under controlled laboratory conditions, which do not always reflect real-world climatic operating scenarios. Second, scaling to areas exceeding $10 remains insufficiently explored within the scope of this study. Third, long-term tests (exceeding 2000 h) have not yet been performed.

(12) Future research should focus on:

Optimizing additive compositions, taking into account their interaction with the crystal lattice;
Integrating new barrier materials, including 2D crystals and hybrid polymers;
Developing models that link the microstructure to degradation processes;
Scaling deposition technologies to roll-to-roll lines using continuous quality control.

4.7. Key Conclusions of the Discussion

(13) On the whole, the presented results and their comparison with literature data allow for several key conclusions:

Defect engineering provides both an efficiency boost and a substantial increase in stability;
Interfacial and chemical approaches act synergistically, suppressing different classes of defects;
Scaling remains a challenge, but modern deposition methods yield comparable performance metrics;
Further development requires the integration of multi-component strategies and the transition to industrial technologies.
Thus, the study lays the groundwork for subsequent efforts aimed at increasing the technology readiness level of perovskite solar cells and guiding them toward commercial implementation.

Conclusion

(1) In the presented work, a comprehensive analysis of defect engineering in perovskite solar cells (PSCs) was conducted, incorporating both experimental studies and numerical modeling. The introduction of chemical additives, morphology control, and interface engineering demonstrated a pronounced synergistic effect, as evidenced by a 12–15% increase in device efficiency compared to control samples.

(2) The research demonstrated that chemical engineering (SCN, guanidinium, inorganic salts) effectively passivates vacancies and suppresses deep traps, while structural control (controlled grain growth, 2D capping) reduces bulk defect density and improves morphological uniformity. Interface engineering (SAMs, barrier layers, dipole interlayers) eliminates energy mismatches and stabilizes phase boundaries, preventing charge accumulation and accelerated degradation.

(3) Testing according to ISOS standards (L1, D1, T1) confirmed that defect-engineered devices retain over 85–90% of their initial efficiency after 1000 hours of operation, whereas control samples lose over 40–50%. Simulation of the dependence of Voc and FF on defect density showed an exponential decline in parameters as the trap concentration increased, emphasizing once more the vital importance of comprehensive defect control.

(4) Technology scaling remains a challenge, but modern film deposition methods—blade-coating, slot-die, and roll-to-roll—demonstrate reproducibility while maintaining key characteristics. Although a partial loss of PCE is observed when increasing the area to the cm^2 scale, optimizing drying and crystallization conditions alongside the introduction of interfacial layers allows minimizing these losses, drawing industrial samples closer to laboratory values.

(5) In conclusion, this work proves that comprehensive defect engineering is a universal strategy for enhancing the efficiency and long-term stability of PSCs. These approaches clear the path toward the industrial realization of perovskite technologies and their integration into hybrid architectures (e.g., perovskite–silicon tandems), marking an important step toward achieving sustainability goals in the field of renewable energy.

References

1. NREL Best Research-Cell Efficiency Chart. National Renewable Energy Laboratory. Available online: https://www.nrel.gov/pv/cell-efficiency.html (accessed January 2025).
2. Park, N.-G. Perovskite solar cells: an emerging photovoltaic technology. *Materials Today* **2015**, 18(2), 65–72. https://doi.org/10.1016/j.mattod.2014.07.007
3. Jeon, N. J.; Na, H.; Jung, E. H.; et al. A fluorene-terminated hole-transporting material for highly efficient and stable perovskite solar cells. *Nature Energy* **2018**, 3, 682–689. https://doi.org/10.1038/s41560-018-0200-6
4. Zhang, W.; Saliba, M.; Stranks, S. D.; et al. Enhancement of perovskite-based solar cells by using a chlorine-based additive. *Nature Communications* **2015**, 6, 6142. https://doi.org/10.1038/ncomms7142
5. Abate, A.; Leijtens, T.; Pathak, S.; et al. Lithium salts as "redox active" p-dopants for organic semiconductors and their impact on the performance of perovskite solar cells. *Energy & Environmental Science* **2014**, 7(10), 3319–3324. https://doi.org/10.1039/C4EE01755H
6. Bu, T.; Li, J.; Zheng, F.; et al. Universal passivation strategy to slot-die printed perovskite solar cells for module integration. *Nature Communications* **2018**, 9, 4609. https://doi.org/10.1038/s41467-018-07027-5
7. Hou, Y.; Aydin, E.; De Bastiani, M.; et al. Efficient tandem solar cells with solution-processed perovskite on textured crystalline silicon. *Science* **2020**, 367(6482), 1135–1140. https://doi.org/10.1126/science.aba3433
8. Snaith, H. J. Present status and future prospects of perovskite photovoltaics. *Nature Materials* **2018**, 17, 372–376. https://doi.org/10.1038/s41563-018-0071-z
9. Zhao, Y.; Zhu, K. Organic–inorganic hybrid lead halide perovskites for optoelectronic and electronic applications. *Chemical Society Reviews* **2016**, 45(3), 655–689. https://doi.org/10.1039/C4CS00458B
10. Jiang, Q.; Zhao, Y.; Zhang, X.; et al. Surface passivation of perovskite film for efficient solar cells. *Nature Photonics* **2019**, 13, 460–466. https://doi.org/10.1038/s41566-019-0398-2